Structural Integrity Associates, Inc.®

5215 Hellyer Ave.
Suite 210
San Jose, CA 95138-1025
Phone: 408-978-8200
Fax: 408-978-8964
www.structint.com
clohse@structint.com

May 14, 2015
Report No. 1400669.401.R0
Quality Program: ☒ Nuclear (Safety-related) ☐ Commercial

Mr. Keith Smith
Entergy Nuclear Operations, Inc.
Palisades Nuclear Plant
27780 Blue Star Memorial Highway
Covert, MI 49043

Subject: Evaluation of the Palisades Nuclear Plant Branch Line Nozzles for Primary Water Stress Corrosion Cracking

Dear Keith:

In Relief Request RR 4-18 [1], Entergy Nuclear Operations (Entergy) committed to volumetrically examine a total of nine (9) pressure retaining dissimilar metal welds (DMWs) containing Alloy 600 nozzles and Alloy 182 weld material at the Palisades Nuclear Plant (Palisades) during the upcoming 1R24 refueling outage (Fall of 2015). Of the nine weld locations, eight are cold leg nozzles (three 2-inch diameter drain nozzles, one 2-inch diameter letdown nozzle, two 2-inch diameter charging nozzles, and two 3-inch diameter spray nozzles) and one 2-inch diameter hot leg drain nozzle.

On December 1, 2014, Entergy contracted with Structural Integrity Associates, Inc. (SI) [2] to support a flaw readiness evaluation for the 1R24 examinations of the nine reactor coolant system (RCS) branch connection Alloy 600 nozzle boss welds at Palisades. SI began working in earnest on this project in early January 2015. The base work scope involved performing flaw evaluations for the hot leg and cold leg branch line DMWs. SI's work was interrupted in mid-February 2015 to support a possible relief request to defer inspections for the upcoming outage.

To support Entergy's new Relief Request, SI was requested to provide a technical basis for deferral of inspection of the hot leg drain nozzle and eight cold leg branch line nozzle DMWs. In order to perform the necessary flaw evaluations, finite element models were developed for the hot leg and cold leg nozzles. These models were used to perform weld residual stress evaluations and calculations of stress intensity factors in the DMWs. Utilizing these new stress intensity factor distributions for postulated circumferential and axial flaws in the DMWs, crack growth due to primary water stress corrosion cracking (PWSCC) was evaluated for both the hot

leg and cold leg configurations. Crack growth durations were then plotted on charts to show the service life of the hot leg and cold leg configurations based on crack growth from an assumed initial flaw depth of 0.025 inch.

This report summarizes the evaluation results. It should be noted that PWSCC was the only crack growth mechanism considered in this evaluation (i.e., PWSCC growth of a postulated axial and circumferential flaw in the weld). The overall goal of SI's evaluation was to show that it takes considerable time to grow postulated flaws to allowable flaw sizes in both the hot leg drain nozzle and the cold leg nozzle configurations, and that the crack growth time for these locations is quite significant.

Finite Element Analyses

For the hot leg drain nozzle, a three-dimensional (3-D) finite element model was developed using the ANSYS software [3]. The area of interest was the nozzle-to-hot leg DMW. The model used elastic-plastic material properties intended for weld residual stress analysis. The model included a local portion of the hot leg pipe and cladding, the drain nozzle, and the nozzle-to-hot leg DMW, including the inside diameter (ID) patch weld, as shown in Figure 1. As depicted in the figure, a single 90° quadrant of the drain nozzle penetration is modeled due to geometric symmetry. The included portion of the hot leg piping measured 36 inches longitudinally and 180 degrees circumferentially. The mesh of the finite element model is shown in Figure 2.

For the cold leg nozzles, one bounding 3-D finite element model was developed using the ANSYS software [4]. All three nozzle configurations (i.e., drain/letdown, charging, and spray) are of similar size (diameter) near the forging boss area (within 1/16 inch). Therefore, the largest ID and smallest outside diameter (OD) of the three nozzle types was chosen for the bounding model. The spray and drain/letdown nozzles have identical nozzle and boss OD dimensions of 4-9/16 inches and 6-3/16 inches, respectively, which are slightly smaller than the charging nozzle OD dimensions of 4-5/8 inches and 6-1/4 inches. For the nozzle ID, the charging nozzle was bored out to 2-5/8 inches in the first 1.5 inches to accommodate a thermal sleeve. For conservatism, it was assumed that the entire nozzle ID is 2-5/8 inches. Therefore, the ID of the bored out charging nozzle and the OD of the spray/drain/letdown nozzles were used for the bounding cold leg nozzle configuration.

For the cold leg nozzles, the area of interest was the nozzle-to-cold leg DMW. The model used elastic-plastic material properties intended for weld residual stress analysis. The model included a local portion of the cold leg pipe and cladding, the nozzle, and the nozzle-to-cold leg DMW, including the ID patch weld, as shown in Figure 3. As depicted in the figure, a single 90° quadrant of the nozzle penetration is modeled due to geometric symmetry. The included portion of the cold leg piping measured 36 inches longitudinally and 180 degrees circumferentially. The mesh of the finite element model is shown in Figure 4.

Weld Residual Stress Analyses

Weld residual stress analyses were performed for the hot leg drain nozzle [5] and bounding cold leg nozzle [6], and the following steps of initial construction were simulated in the analyses:

1. Deposit cladding on hot leg/cold leg pipe inside surface.
2. Install nozzle, backing ring, and deposit boss weld.
3. Remove backing ring and deposit ID patch weld.
4. Post weld heat treatment (PWHT), including creep effects based upon experimental data.
5. Subject the configuration to a hydrostatic test.
6. Impose five cycles of "shakedown" at normal operating temperature and pressure to stabilize the residual stress fluctuations due to stress redistribution.

For the hot leg drain nozzle, the boss weld connects the drain nozzle to the hot leg piping. As shown in Figure 5, the weld is composed of 40 nuggets deposited in 20 weld layers. As depicted in Figure 6, the ID patch weld is composed of 6 nuggets deposited in 2 layers. Stabilized stress results normal to a circumferential flaw are shown in Figure 7, and those normal to an axial flaw are shown in Figure 8. They represent the operating conditions of the hot leg, and include the residual stresses due to welding plus the operating pressure of 2085 psig and steady-state temperature of 583°F.

For the cold leg nozzles, the boss weld connects the bounding nozzle to the cold leg piping. As shown in Figure 9, the weld is composed of 40 nuggets deposited in 20 weld layers. As depicted in Figure 10, the ID patch weld is composed of 6 nuggets deposited in 2 layers. Stabilized stress results normal to a circumferential flaw are shown in Figure 11, and those normal to an axial flaw are shown in Figure 12. . They represent the operating conditions of the cold leg, and include the residual stresses due to welding plus the operating pressure of 2085 psig and steady-state temperature of 537°F.

Crack Growth Evaluations

Crack growth evaluations were performed for the hot leg drain nozzle [7] and the bounding cold leg nozzle [8]. For both the hot leg drain nozzle and bounding cold leg nozzle, stress intensity factors (Ks) at five depths for a 360° inside surface connected, part-through wall circumferential flaw as well as two axial thumbnail flaws, at the 0- and 90-degree azimuthal locations of the nozzle, were calculated using finite element analysis techniques. For the circumferential flaw, the maximum K values around the nozzle circumference for each flaw depth were extracted and used as input for performing the PWSCC growth analyses. For the axial flaws, the K at the deepest point of the thumbnail shape was used as input for performing the PWSCC growth analyses.

For the crack growth analyses, a small initial flaw size of 0.025 inch was chosen. This is based on the expected flaw size that would be possible since the crack growth evaluation is assumed to

start on day one of plant operation. The final flaw size for these analyses is 75% of the wall thickness. This final depth is chosen as it is the maximum allowable flaw depth per Section XI of the ASME Code for pipe flaw evaluations. The 75% requirement is driven by the tables and equations in Appendix C, Article C-5000 of Section XI of the ASME Code. The equations and tables are limited to 75% of the pipe thickness. The values for a through-wall flaw (95% depth) are also calculated to explore the time for a flaw to grow through-wall. In response to Nuclear Regulatory Commission RAI's [12] pertaining to Relief Request RR 4-18 [1], SI performed limit load analyses to show that the hot leg/cold leg/nozzle structures remained structurally stable for both circumferential and axial through-wall flaws.

The key parameters used in the crack growth calculations included:

- Initial flaw depth = 0.025" for both hot and cold leg configurations
- Temperature = 583°F (hot leg) and 537°F (cold leg)
- Wall thickness = 4" (hot leg pipe thickness) and 3" (cold leg pipe thickness)

An example of the 360° circumferential flaw is shown in Figure 13 for the hot leg nozzle and Figure 18 for the bounding cold leg nozzle. A total of five circumferential flaw depths were modeled. Similarly, five axial flaw depths were modeled at the 0- and 90-degree azimuths. Figure 14 shows the axial flaws modeled at the 0-degree azimuth for the hot leg nozzle, and Figure 19 shows the comparable axial flaws modeled for the bounding cold leg nozzle.

Stress intensity factors, Ks, were calculated for the 360° circumferential flaws as well as the axial flaws at the 0° and 90° locations. The stress intensity factors were calculated using the stress distributions for residual stress plus normal operating conditions shown in Figures 7 and 8 for the hot leg drain nozzle, and Figures 11 and 12 for the bounding cold leg nozzle. In addition, a far field in-plane bending moment is applied to the free end of the hot leg and cold leg run piping to account for piping moments in the main loop piping. This combined loading is used for the determination of the stress intensity factors for both the circumferential and axial flaws. Figures 15 and 16 show the calculated stress intensity factors for the hot leg drain nozzle for the circumferential and axial flaws, respectively. Figures 20 and 21 show the calculated stress intensity factors for the bounding cold leg nozzle for the circumferential and axial flaws, respectively.

Crack growth evaluations were performed for all three flaws. For the hot leg drain nozzle, Figure 17 shows that the time for an initial 0.025" deep flaw to grow to 75% through wall is 30.5 years for the bounding axial flaw (on the 0° plane) and 33.9 years for the circumferential flaw. For the 100% through wall flaw (growth up to 95%) the bounding axial flaw takes 36.7 years (on the 0° plane) and the circumferential flaw takes 42.1 years as shown in Figure 17.

For the bounding cold leg nozzle, Figure 22 shows that the time for an initial 0.025" deep flaw to grow to 75% through wall is 64.5 years for the bounding axial flaw (on the 0° plane) and 55.6 years for the circumferential flaw. For the 100% through wall flaw (growth up to 95%) the

bounding axial flaw takes 77.0 years (on the 0° plane) and the circumferential flaw takes 66.2 years as shown in Figure 22.

Potential Additional Margin Due to PWHT

Dominion Engineering documented in Reference 9 that industry papers [10, 11] note a benefit in fatigue crack growth rate when Alloy 182 weld metal underwent PWHT. This benefit ranged from a factor of two to four. There was a recommendation that crack growth rates be reduced by a factor of two based on this data. If such a factor were used for the nozzles at Palisades, it would increase the crack growth times previously discussed. For comparison, only the bounding crack growth life will be discussed here. This is the axial flaw for the hot leg drain nozzle, and the circumferential flaw for the cold leg nozzles. A factor of two would increase the limiting hot leg drain nozzle duration to 61.0 years, and the bounding cold leg nozzle to 111.2 years for flaws to grow 75% through wall. Similarly, the durations for 100% through wall flaws (growth up to 95%) would increase to 73.4 years for the hot leg drain nozzle and 132.4 years for the cold leg nozzle.

Crack Initiation Time

The original relief request [1] did not include any consideration for crack initiation. Attachment A of this report includes a calculation of the initiation time for the hot leg drain nozzle and cold leg bounding nozzle using one of the models in the xLPR program that was developed by EPRI. The calculation of initiation time based on the Palisades results shows that the time to initiation for the hot leg drain nozzle is approximately 130 years. Attachment A contains additional details regarding the calculation. Combining crack initiation time with the PWHT reduction in crack growth rate, the time for a flaw to grow to 75% through wall will approach 200 years for the hot leg drain nozzle. Using the crack initiation value for the cold leg nozzles, the time for a flaw to grow to 75% through wall would exceed 600 years.

Conclusions

Based on the assessments and calculations documented herein, it is concluded that these welds do not experience fast growing flaws due to PWSCC. The hot leg drain nozzle limiting crack growth life, not considering the benefits of PWHT or crack initiation time, is 30.5 years for a flaw to grow to 75% through wall, and 36.7 years for a flaw to grow to 100% through wall (95% through wall). Similarly, the cold leg nozzles take 55.6 years for the limiting flaw to grow to 75% through wall, and 66.2 years for 100% through wall (95% through wall). The cold leg nozzles lag the hot leg nozzle by roughly a factor of two.

It should be noted that the resulting crack growth times are specified as the duration during which the reactor is at operating pressure and temperature and not simply years since the reactor was licensed to operate. Per Reference 13, the total Effective Full Power Years (EFPY) at the end of the following refueling outage (1R25) is expected to be 28.8, which is less than the 75% through-wall crack growth time for both the hot leg nozzle and bounding cold leg nozzle.

These crack growth lives do not consider the potential additional margin on PWSCC growth rate for PWHT or crack initiation time. Taking into account these margins would increase the time for a crack to grow to 75% or 100% through wall to almost 200 years or more. Based on this information, deferring inspections on these locations for one more plant operating cycle will not represent a decrease in nuclear safety.

References

1. Relief Request Number RR 4-18, "Proposed Alternative, Use of Alternate ASME Code Case N-770-1 Baseline Examination," PNP 2014-015, February 25, 2014.
2. Entergy Nuclear Operations, Inc. Contract Order No. 10426669, Effective Date January 1, 2015.
3. Structural Integrity Associates Calculation 1400669.310, Rev. 0, "Finite Element Model for Hot Leg Drain Nozzle."
4. Structural Integrity Associates Calculation 1400669.320, Rev. 0, "Finite Element Model Development for the Cold Leg Drain, Spray, and Charging Nozzles."
5. Structural Integrity Associates Calculation 1400669.312, Rev. 0, "Hot Leg Drain Nozzle Weld Residual Stress Analysis."
6. Structural Integrity Associates Calculation 1400669.322, Rev. 0, "Cold Leg Bounding Nozzle Weld Residual Stress Analysis."
7. Structural Integrity Associates Calculation 1400669.313, Rev. 0, "Crack Growth Analysis of the Hot Leg Drain Nozzle."
8. Structural Integrity Associates Calculation 1400669.323, Rev. 0, "Crack Growth Analysis of the Cold Leg Bounding Nozzle."
9. Letter from G. White (Dominion Engineering, Inc.) to W. Sims (Entergy), "Effect of Post-Weld Heat Treatment Applied to Alloy 82/182 Full-Penetration Branch Pipe Connection Welds at Palisades," DEI Letter L-4199-00-01, Rev. 0, dated February 25, 2014.
10. T. Cassagne, D. Caron, J. Daret, and Y. Lefèvre, "Stress Corrosion Crack Growth Rate Measurements in Alloys 600 and 182 in Primary Water Loops under Constant Load," *Proceedings of 9th International Symposium on Environmental Degradation of Materials in Nuclear Systems—Water Reactors*, The Minerals, Metals & Materials Society, Warrendale, PA, 1999, pp. 217–224.
11. S. Le Hong, J. M. Boursier, C. Amzallag, and J. Daret, "Measurements of Stress Corrosion Cracking Growth Rates in Weld Alloy 182 in Primary Water of PWR," *Proceedings of 10th International Conference on Environmental Degradation of Materials in Nuclear Power Systems—Water Reactors*, NACE International, 2002.
12. Entergy Nuclear Operation, Inc. letter PNP 2014-028, "Supplemental Response to Request for Additional Information, dated February 26, 2014, for Relief Request Number RR 4-18, Proposed Alternative, Use of Alternate ASME Code Case N-770-1 Baseline Examination," dated March 6, 2014.
13. Email from Daniel Depuydt (Entergy) to Norman Eng (SI), dated May 13, 2015, "Subject: Palisades EFPY at 1R25," includes attached file "WCAP-15353-Suppl 1 Excerpt.pdf," SI File No. 1400669.205.

Very truly yours,

Preparer:

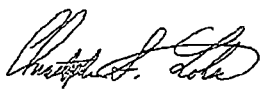

5/14/2015

Chris S. Lohse, P.E.
Senior Consultant

Date

Reviewer:

5/14/2015

Dilip Dedhia
Senior Associate

Date

Reviewer:

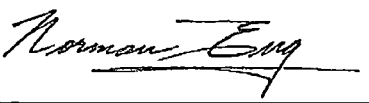

5/14/2015

Norman Eng
Associate

Date

Approver:

5/14/2015

Richard A. Mattson, P.E.
Senior Associate

Date

Attachment A – Crack Initiation Study

cc: R. Bax
M. Fong
C. Fourcade
F. Ku
G. Mukhim
W. Wong

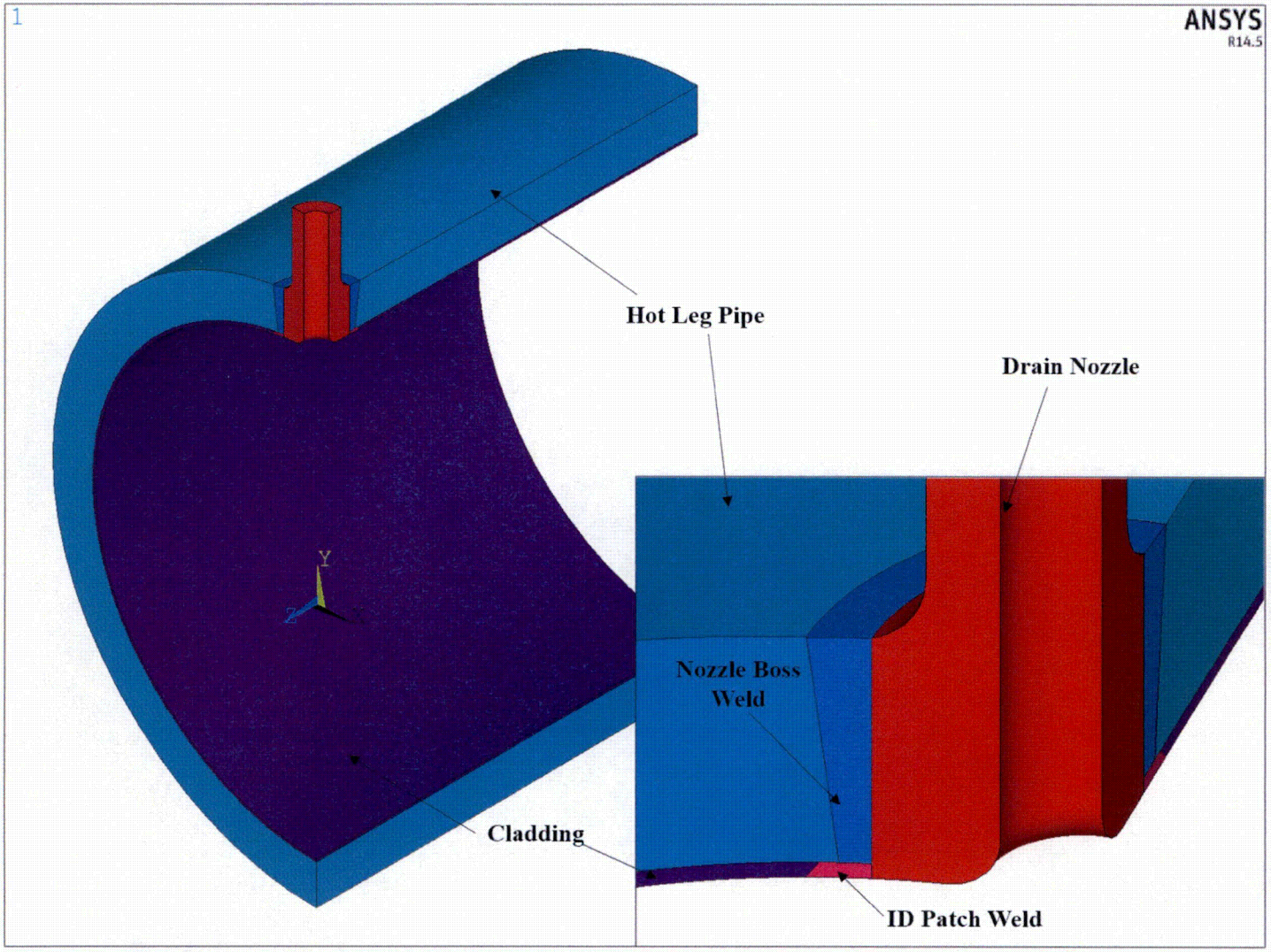

Figure 1. Components Included in the Hot Leg Drain Nozzle Finite Element Model

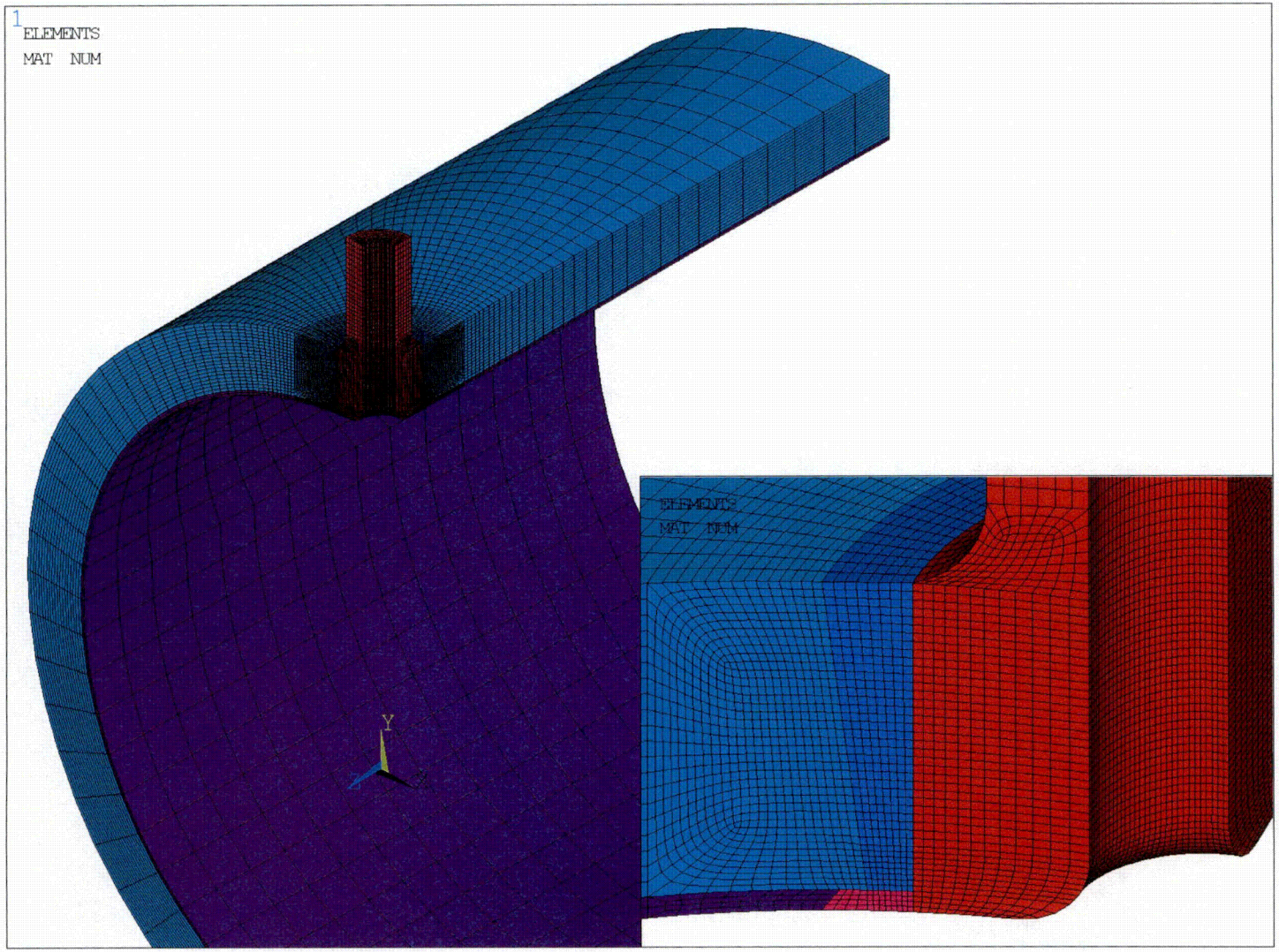

Figure 2. Isometric View of the Hot Leg Drain Nozzle Finite Element Model
Note: Nozzle weld detail is shown in the bottom right corner.

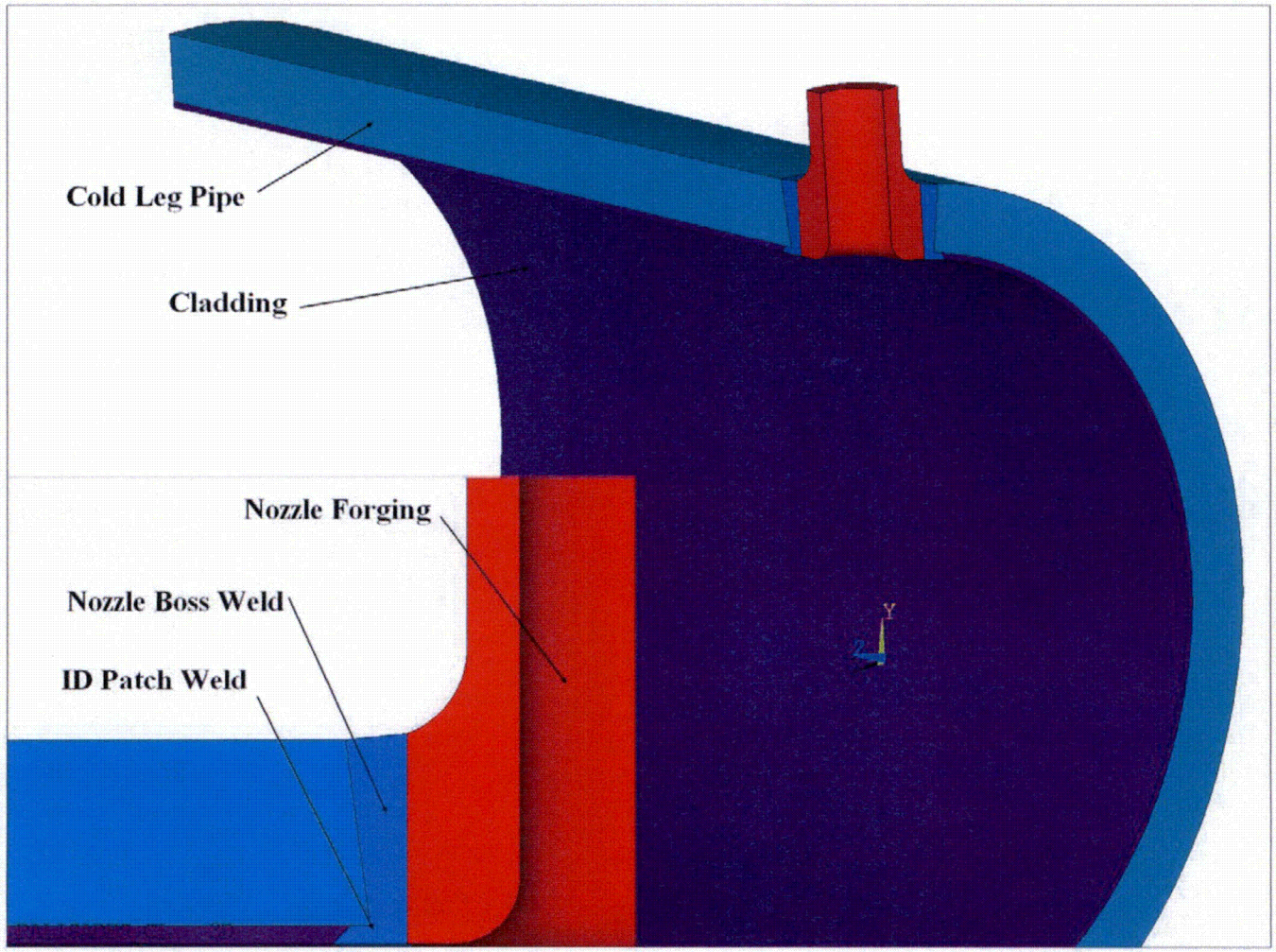

Figure 3. Components Included in the Bounding Cold Leg Nozzle Finite Element Model

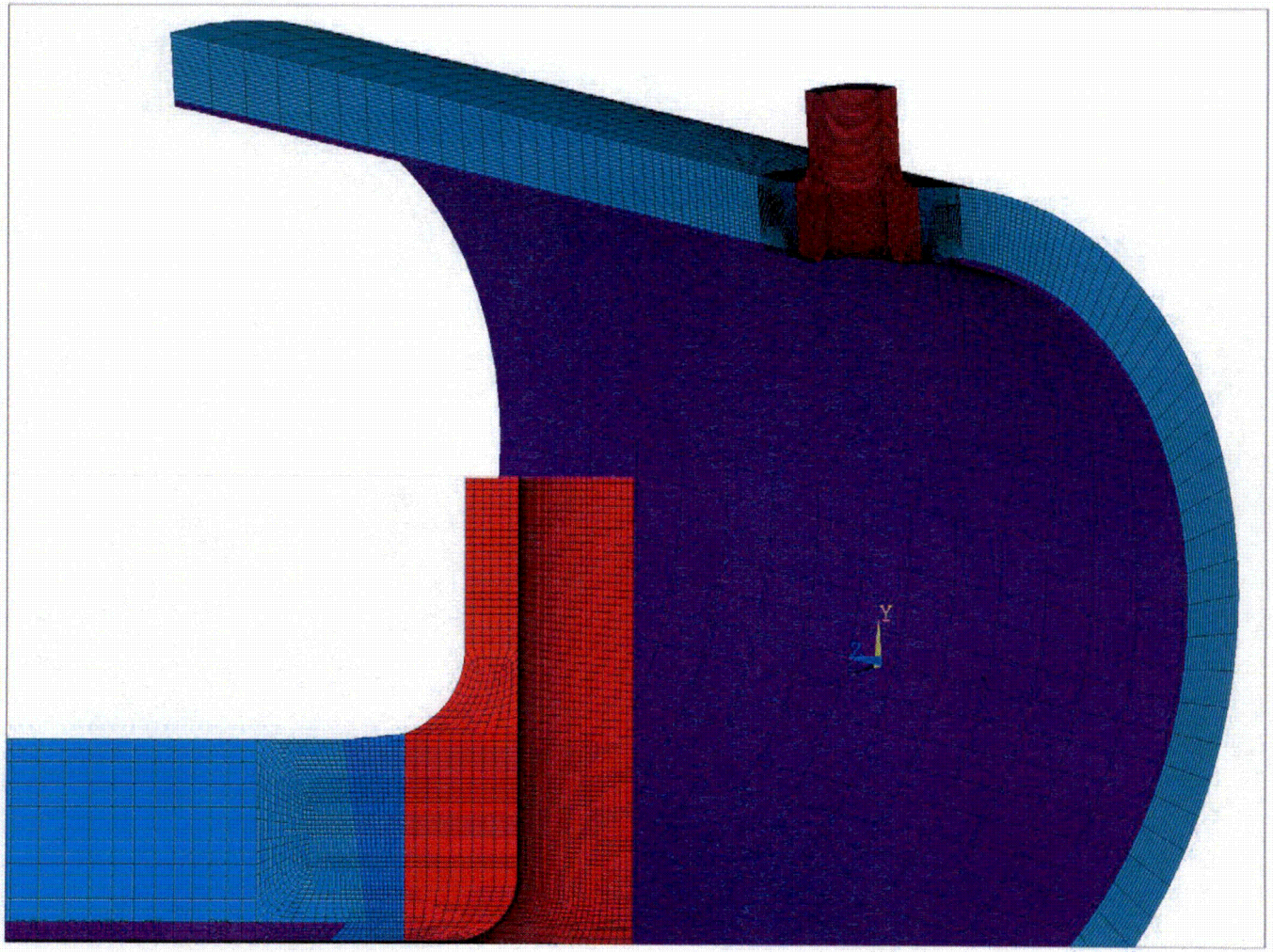

Figure 4. Isometric View of the Bounding Cold Leg Nozzle Finite Element Model
Note: Nozzle weld detail is shown in the bottom left corner.

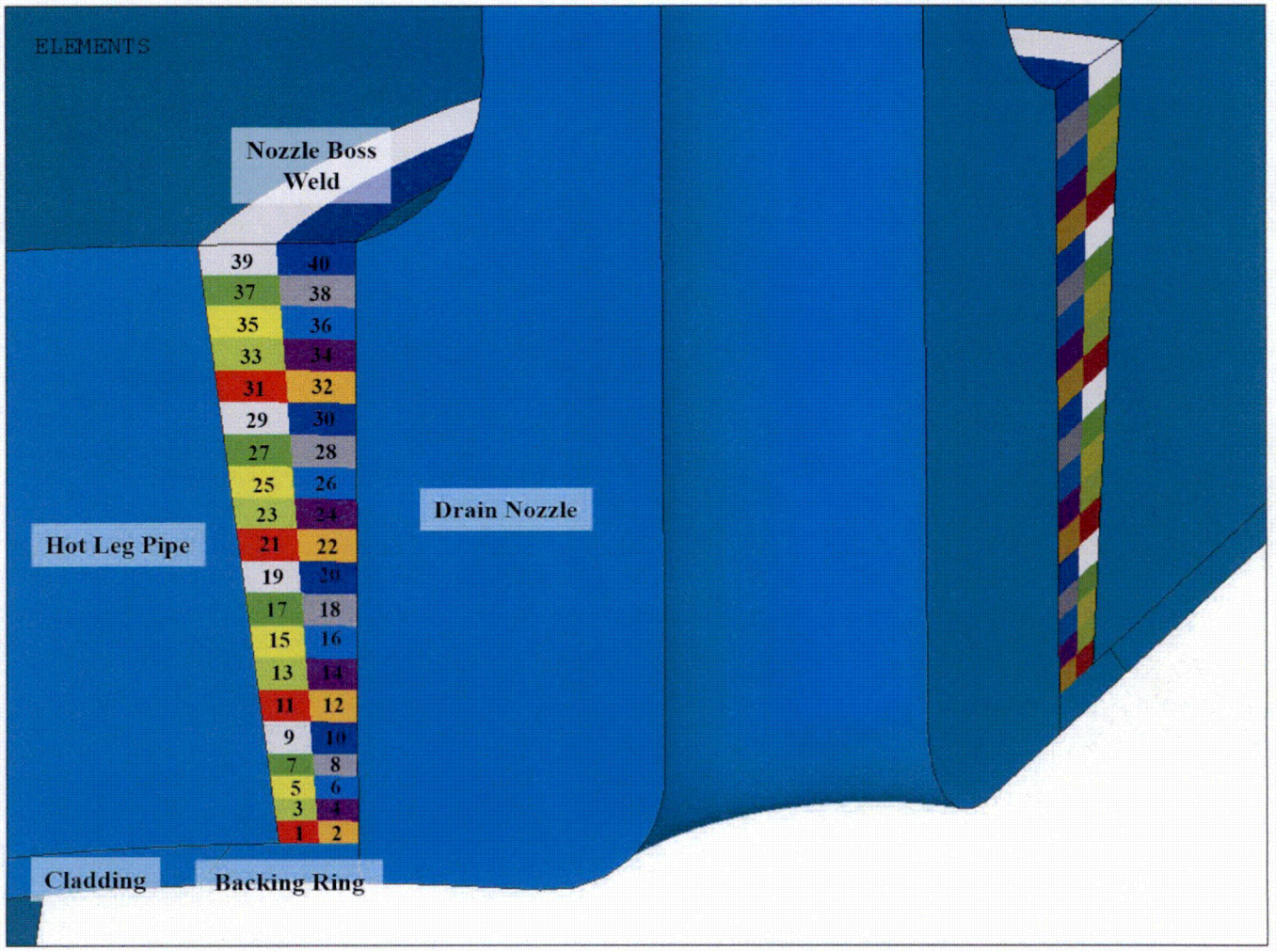

Figure 5. Weld Nugget Definitions for the Hot Leg Drain Nozzle Boss Weld

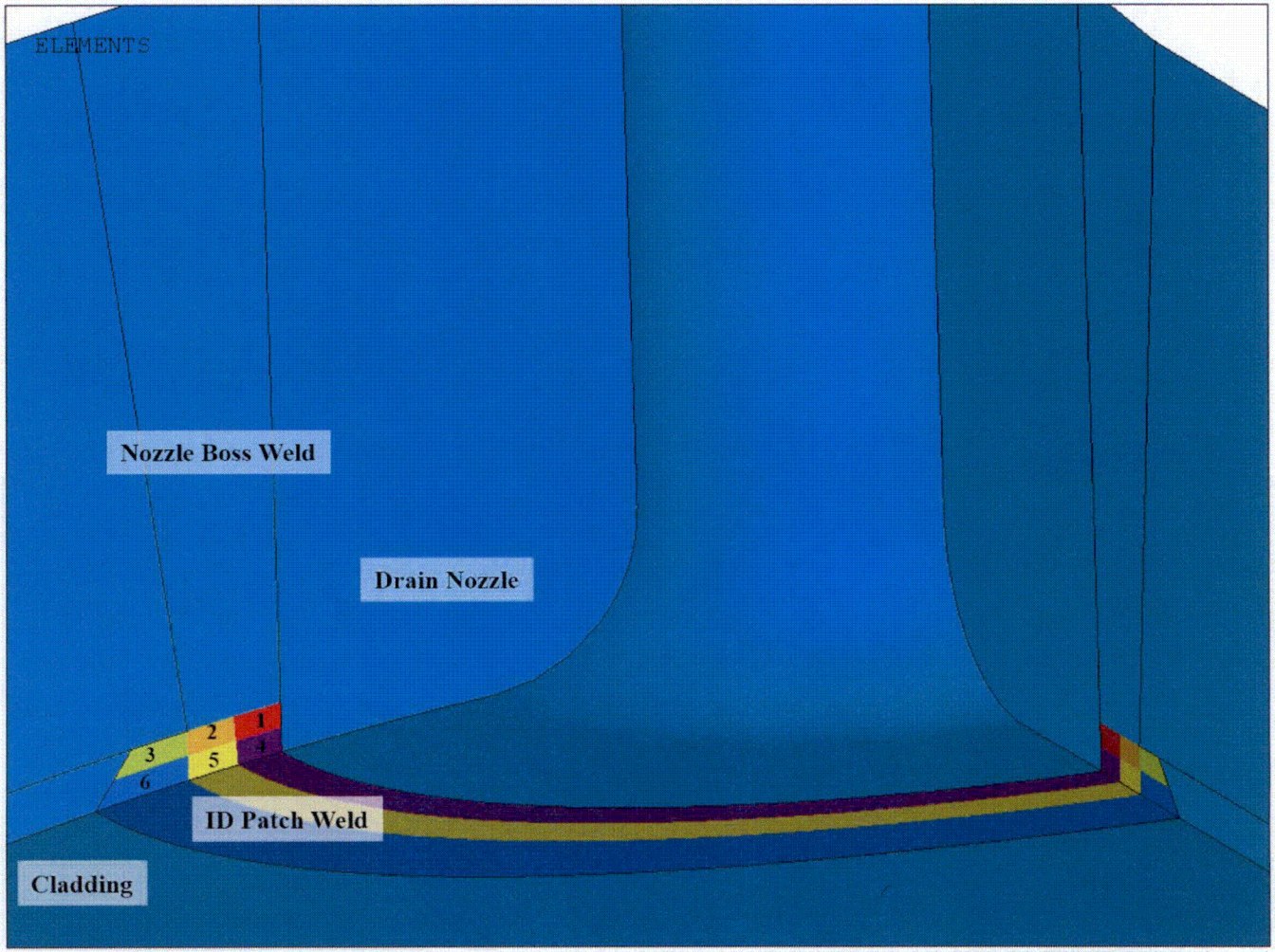

Figure 6. Weld Nugget Definitions for the Hot Leg Drain Nozzle ID Patch Weld

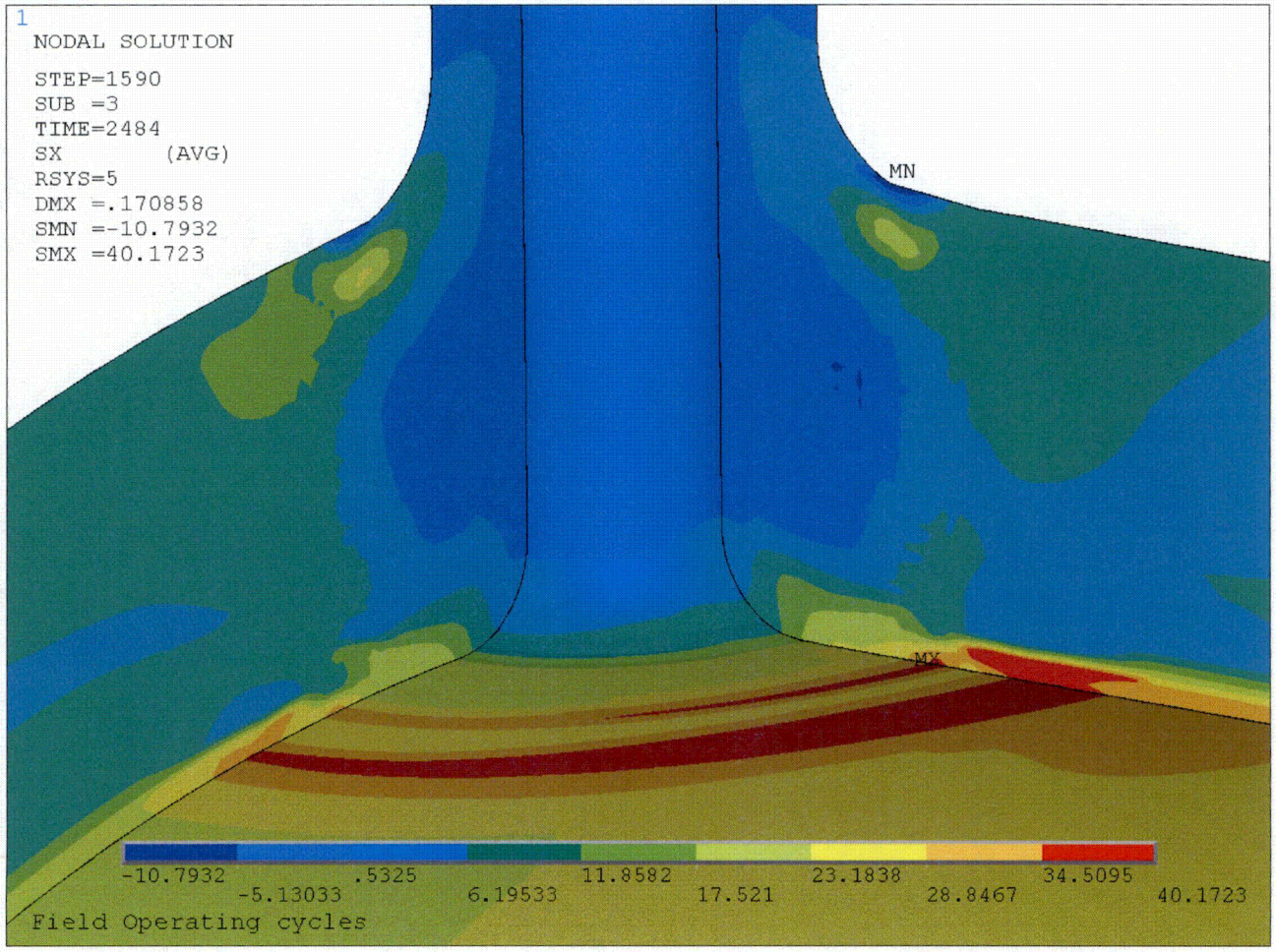

Figure 7. Radial Stresses at Operating Conditions for the Hot Leg Drain Nozzle
Note: Radial stresses are shown in the nozzle axis radial direction and units are in ksi.

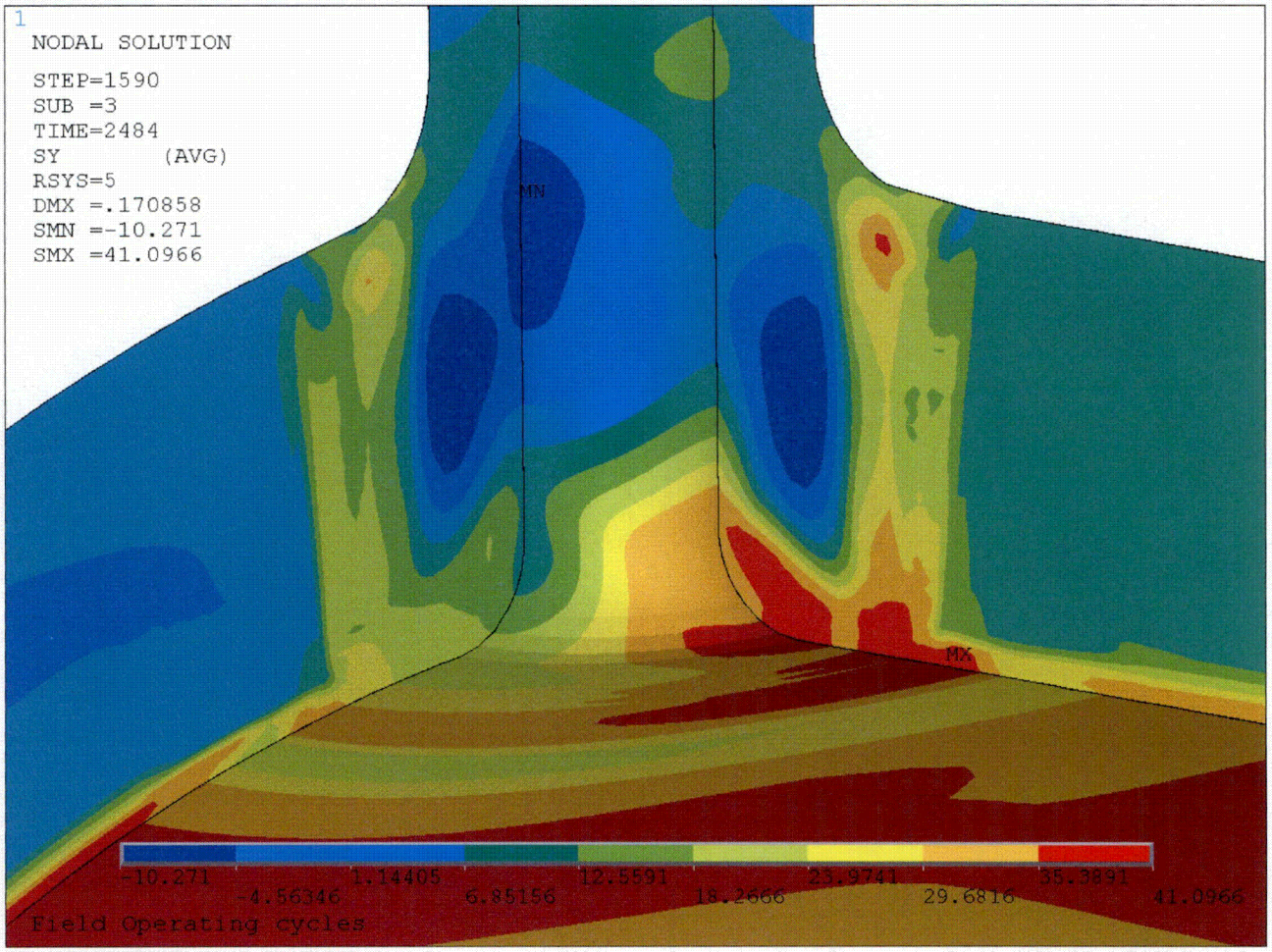

Figure 8. Circumferential Stresses at Operating Conditions for the Hot Leg Drain Nozzle
Note: Circumferential stresses are shown in the nozzle axis circumferential direction and units are in ksi.

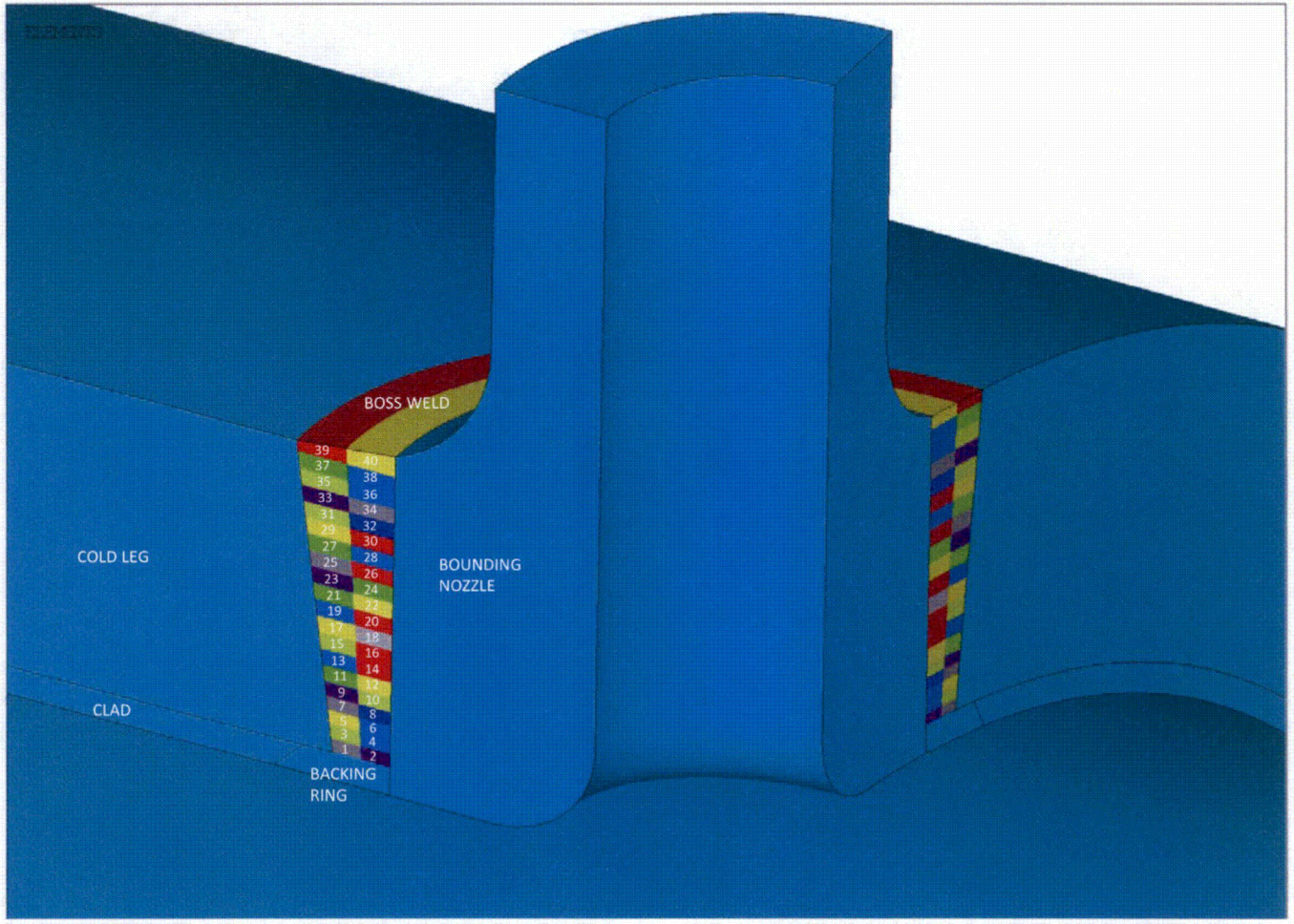

Figure 9. Weld Nugget Definitions for the Bounding Cold Leg Nozzle Boss Weld

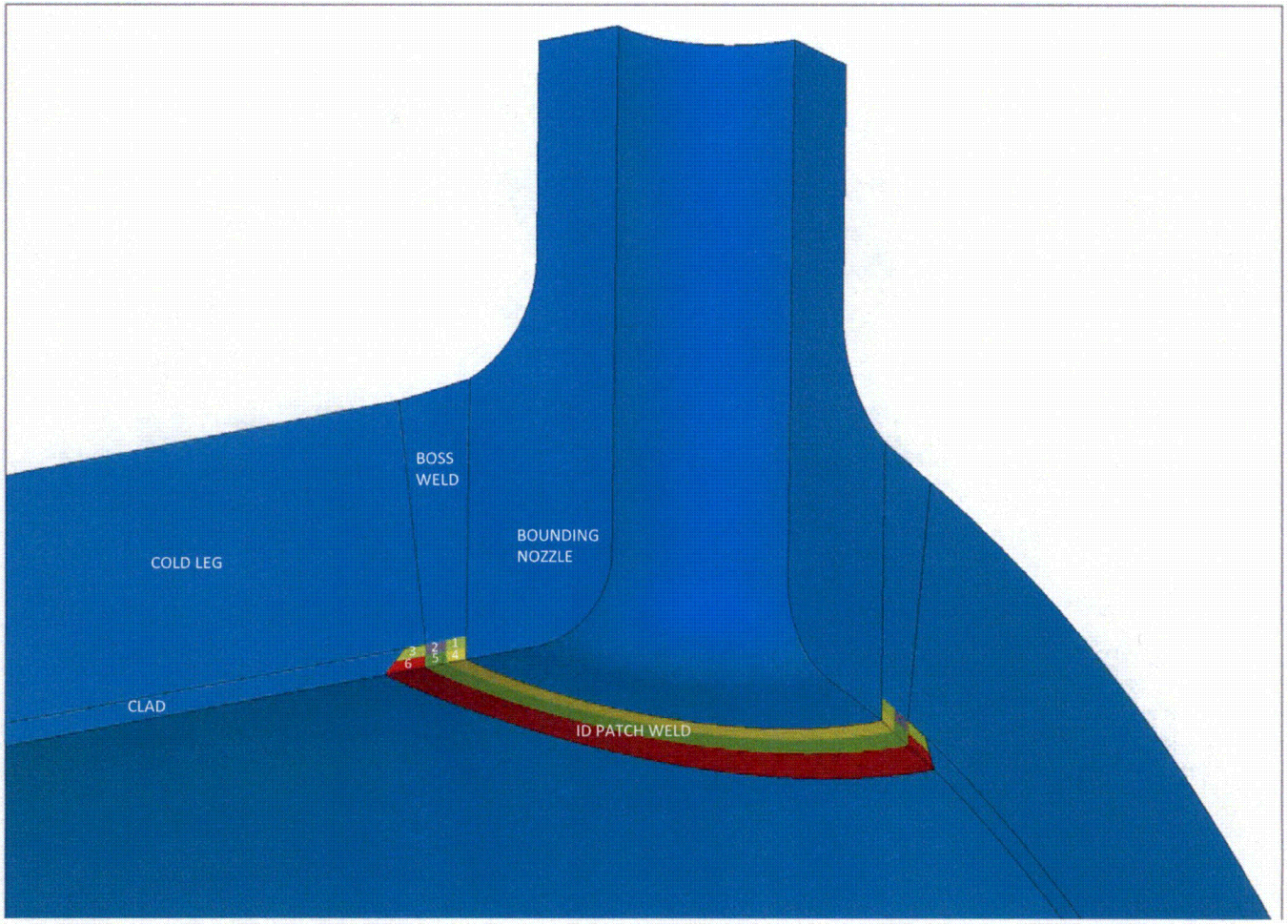

Figure 10. Weld Nugget Definitions for the Bounding Cold Leg Nozzle ID Patch Weld

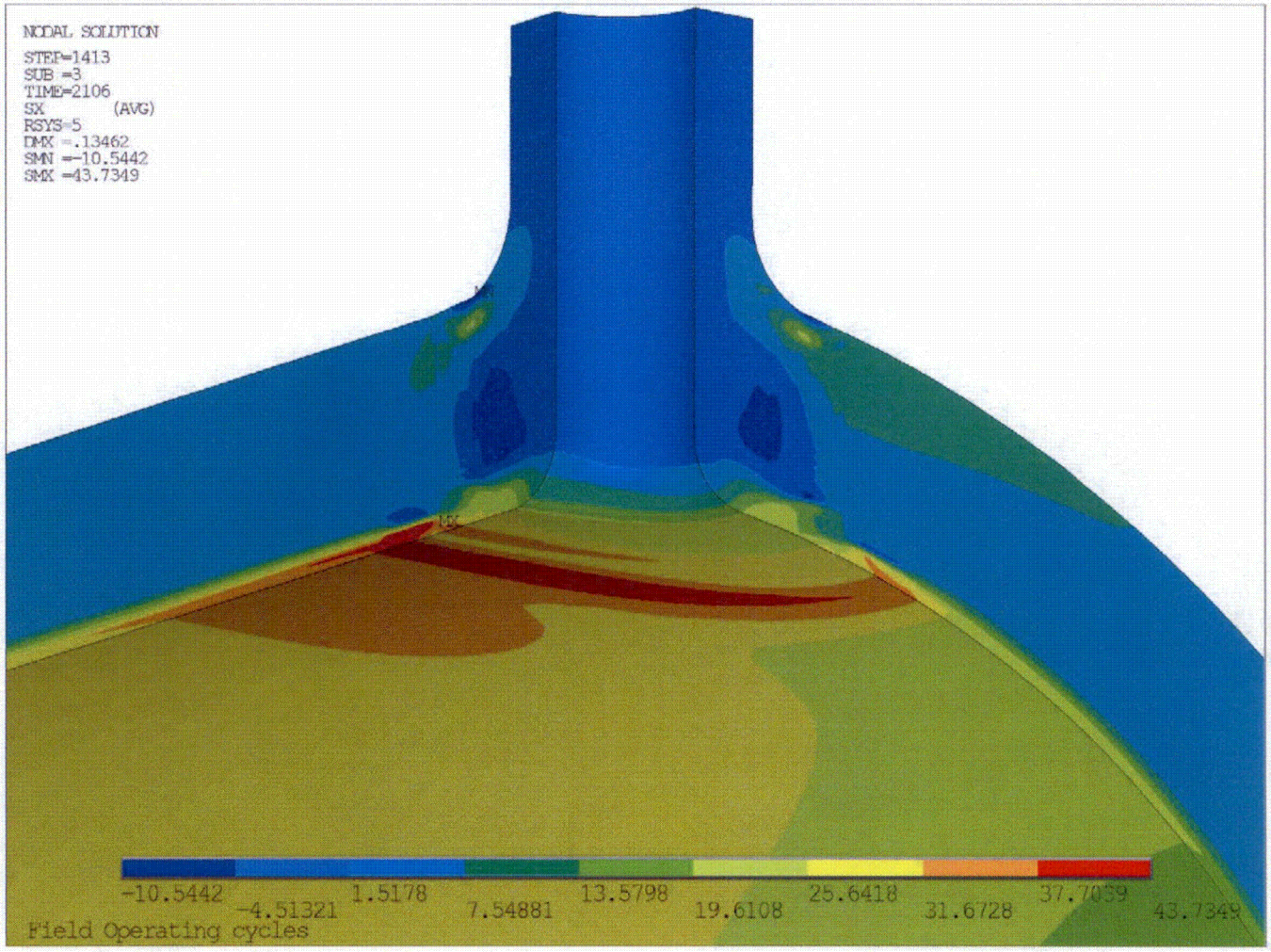

Figure 11. Radial Stresses at Operating Conditions for the Bounding Cold Leg Nozzle
Note: Radial stresses are shown in the nozzle axis radial direction and units are in ksi.

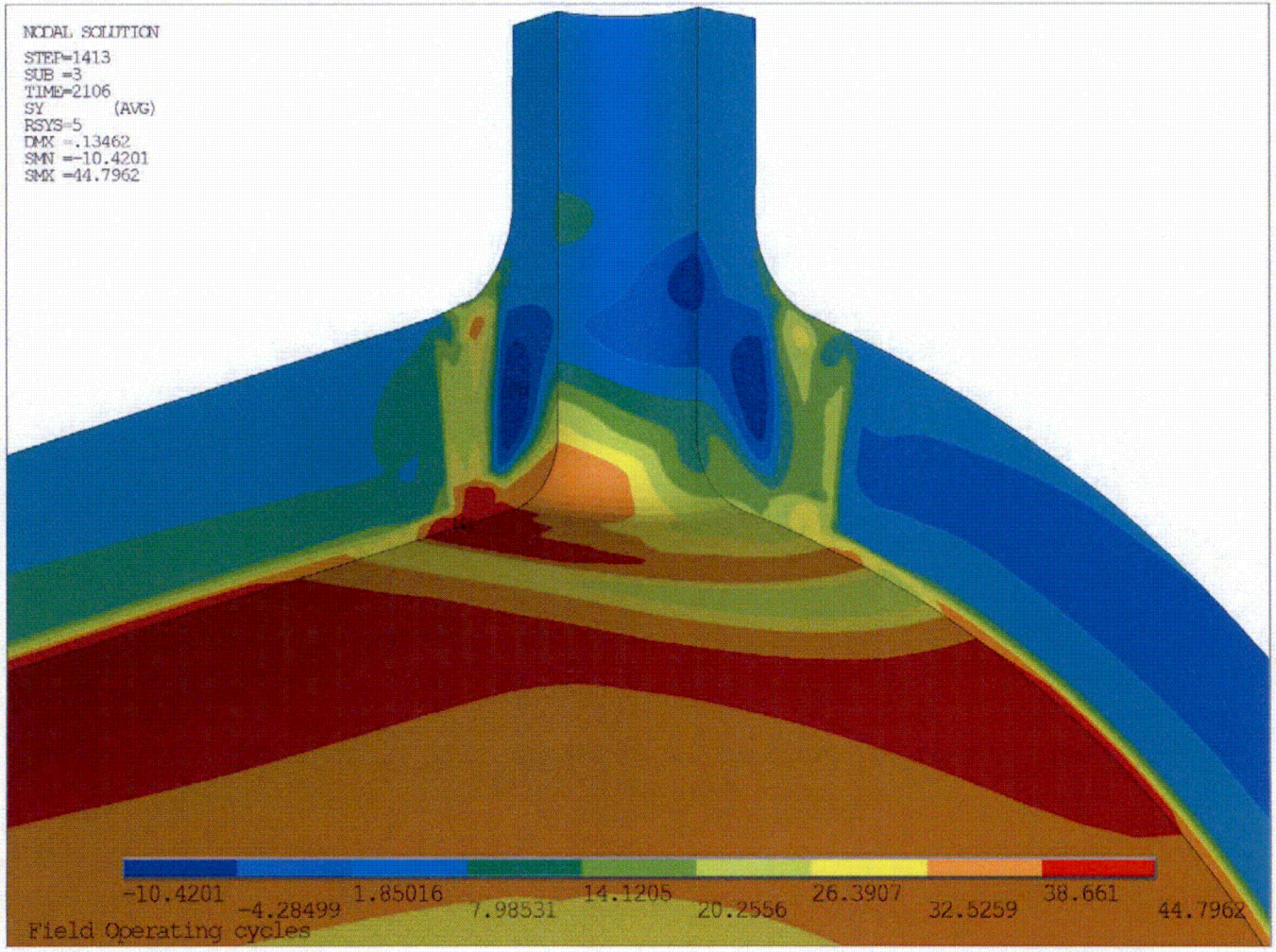

Figure 12. Circumferential Stresses at Operating Conditions for the Bounding Cold Leg Nozzle
Note: Circumferential stresses are shown in the nozzle axis circumferential direction and units are in ksi.

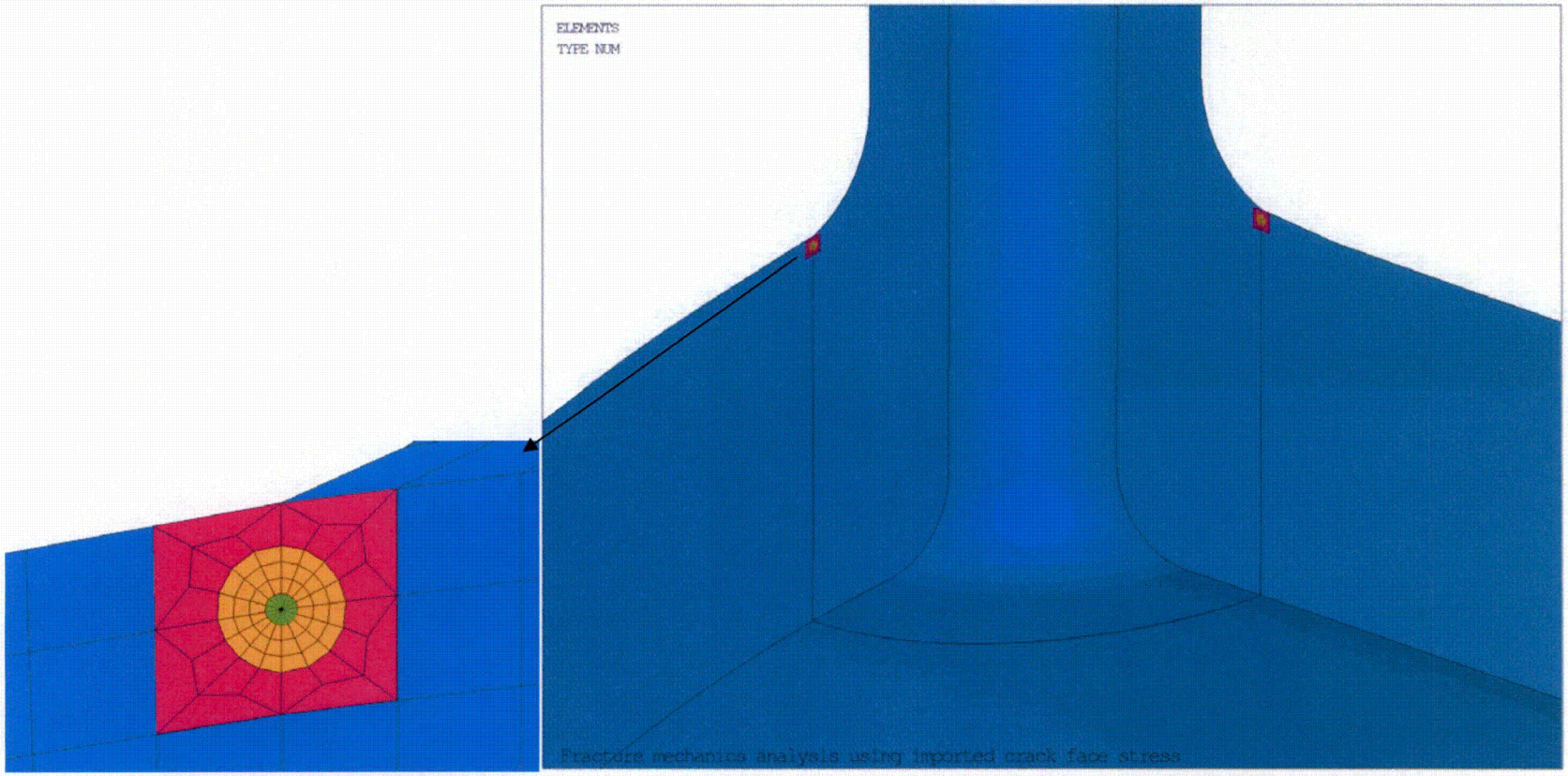

Figure 13. Circumferential Flaw with Crack Tip Elements Inserted for the Hot Leg Drain Nozzle
Note: Deepest circumferential flaw is shown as an example.

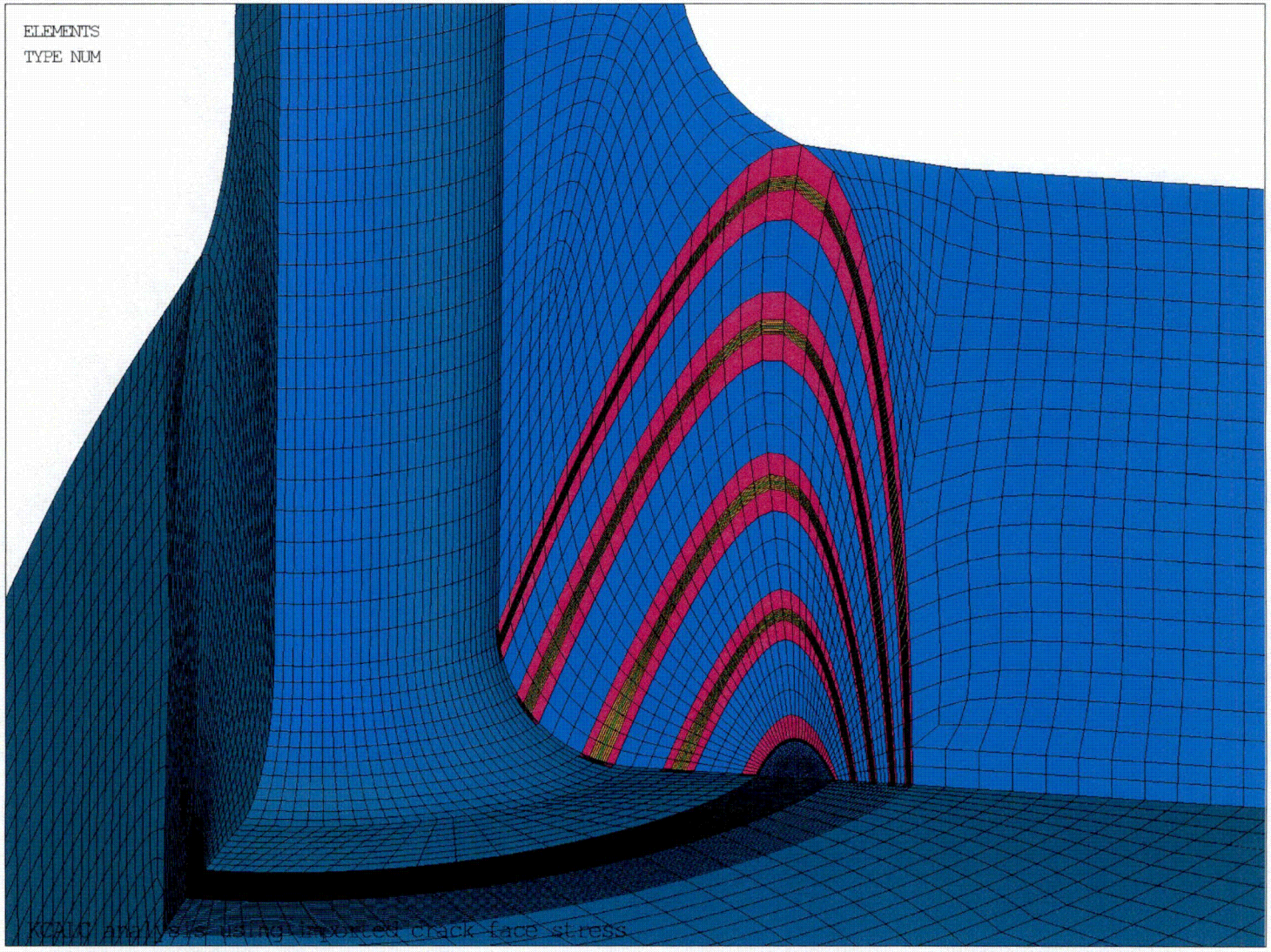

Figure 14. Axial Flaws on the 0° Face with Crack Tip Elements Inserted for the Hot Leg Drain Nozzle
Note: Only the 0° axial flaws are shown. The 90° flaws are similar.

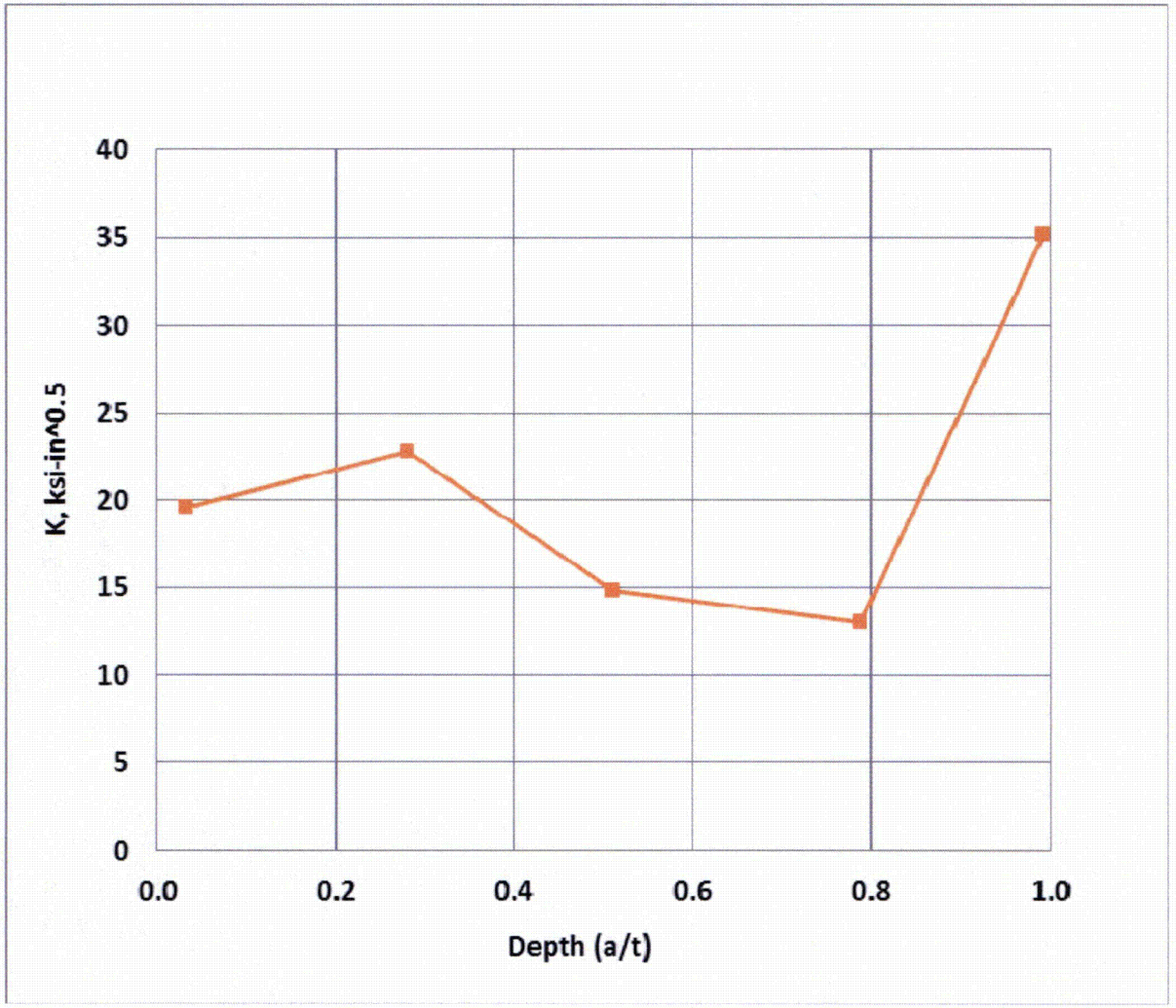

Figure 15. Stress Intensity Factors as a Function of Depth for the Hot Leg Drain Nozzle Circumferential Flaws

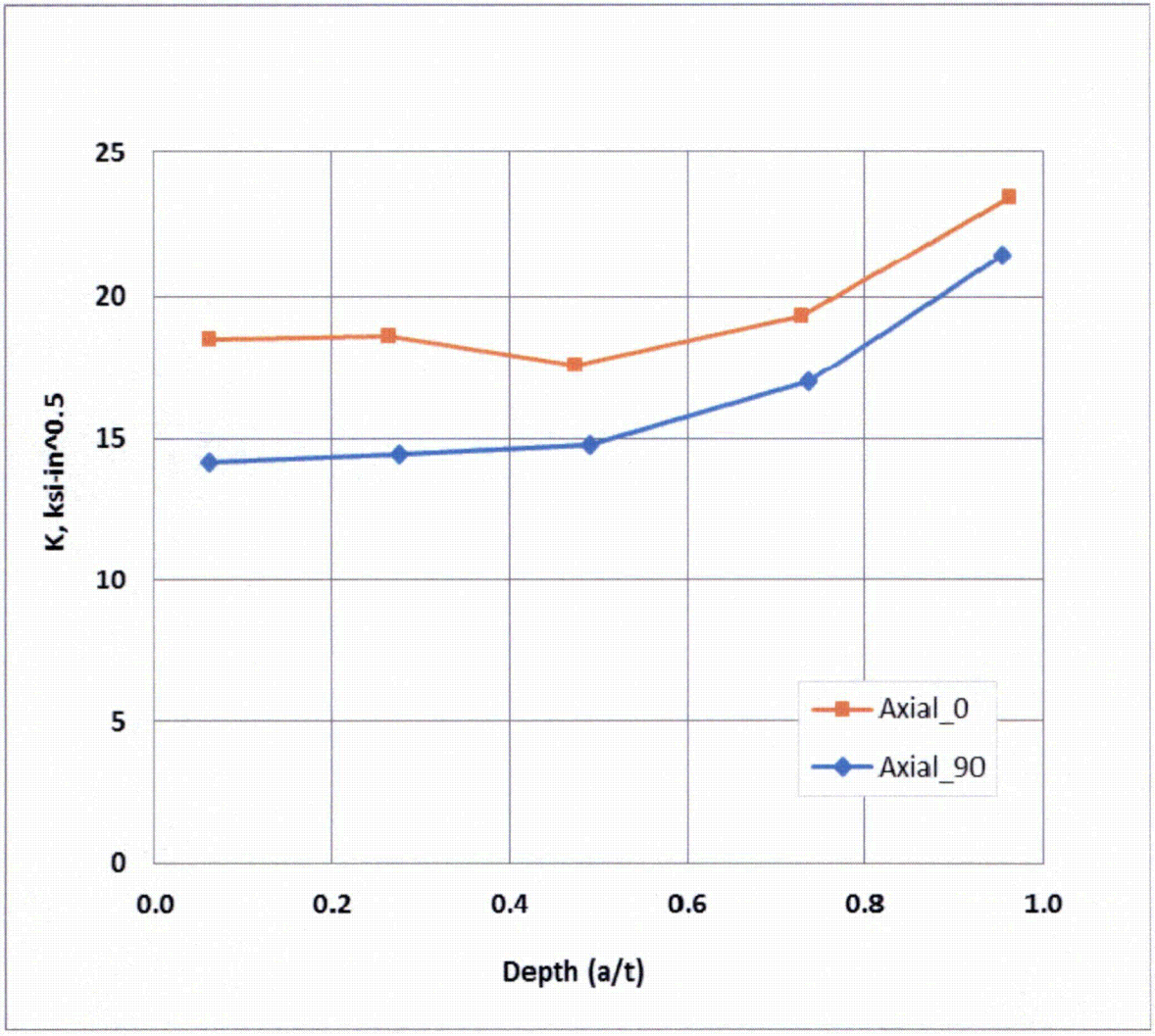

Figure 16. Stress Intensity Factors as a Function of Depth for the Hot Leg Drain Nozzle Axial Flaws

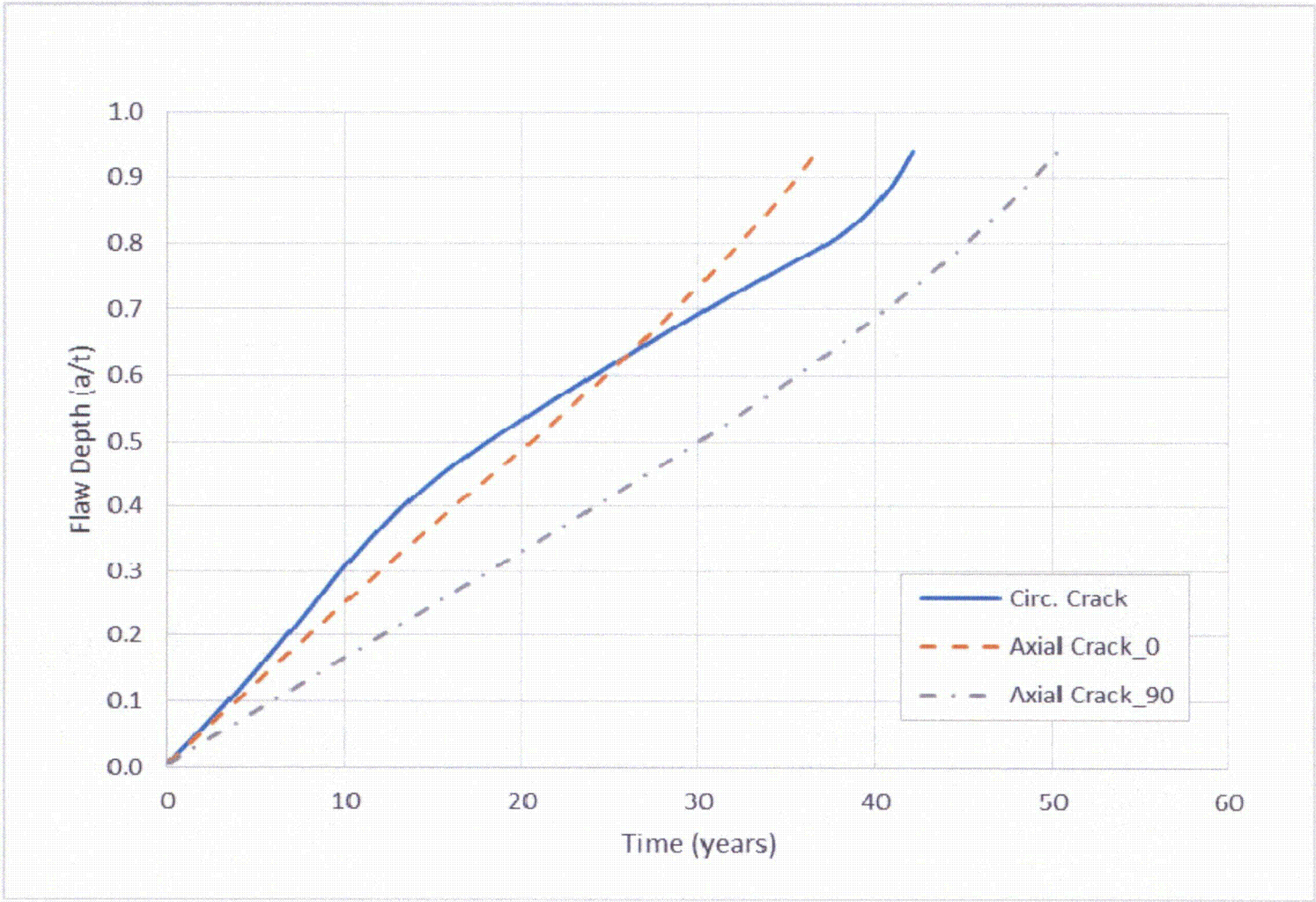

Figure 17. Crack Growth for All Flaw Types in the Hot Leg Drain Nozzle (Initial Flaw of 0.025")

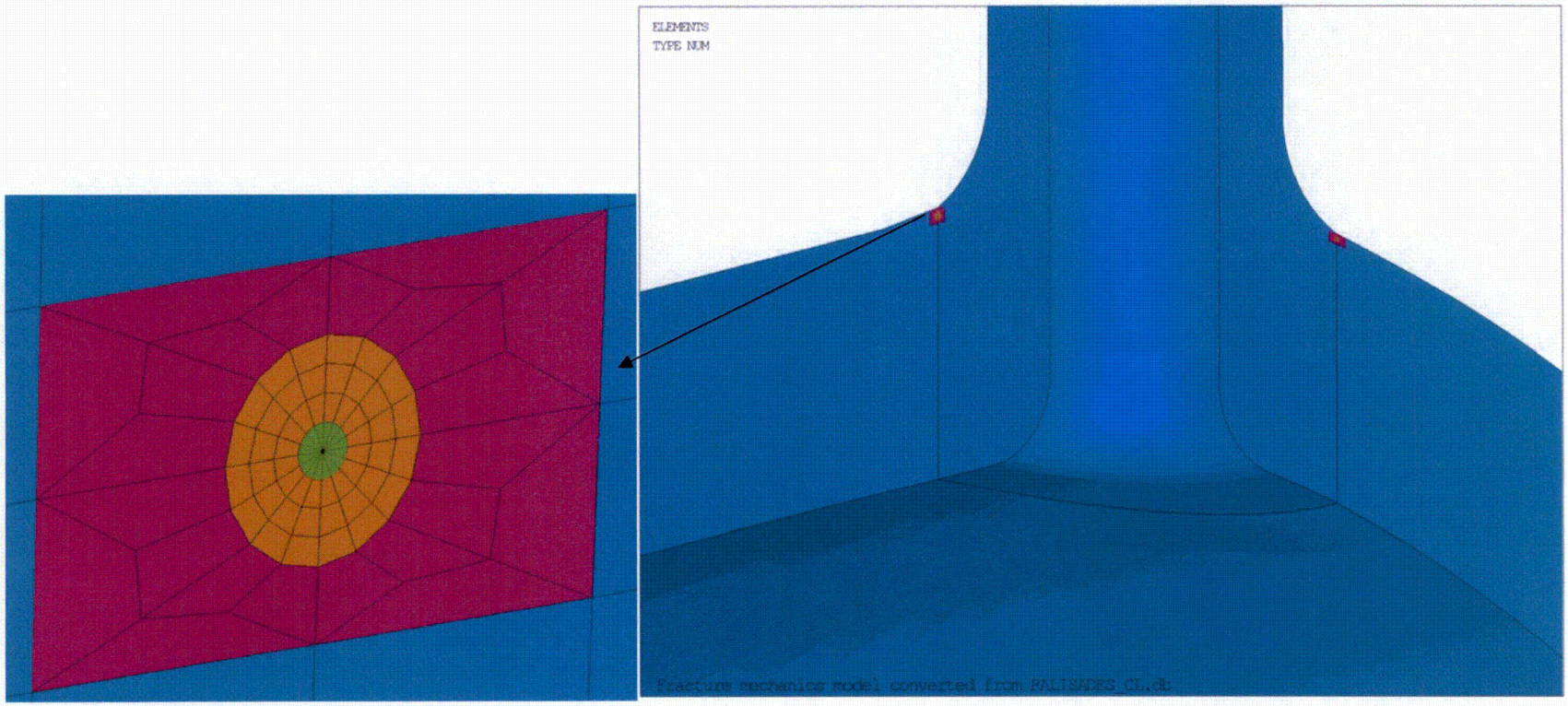

Figure 18. Circumferential Flaw with Crack Tip Elements Inserted for the Bounding Cold Leg Nozzle
Note: Deepest circumferential flaw is shown as an example.

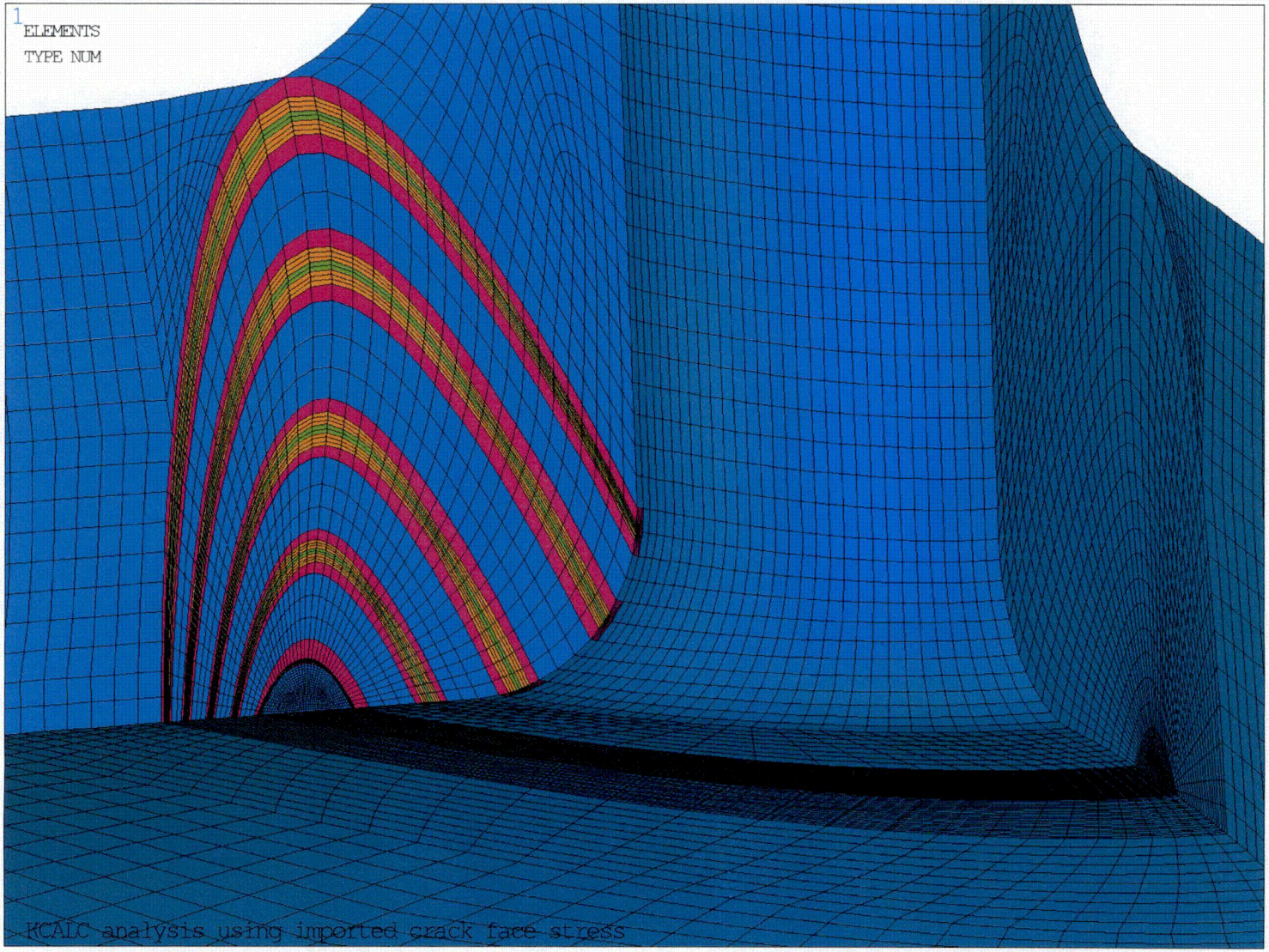

Figure 19. Axial Flaws on the 0° Face with Crack Tip Elements Inserted for the Bounding Cold Leg Nozzle
Note: Only the 0° axial flaws are shown. The 90° flaws are similar.

Figure 20. Stress Intensity Factors as a Function of Depth for the Bounding Cold Leg Nozzle Circumferential Flaws

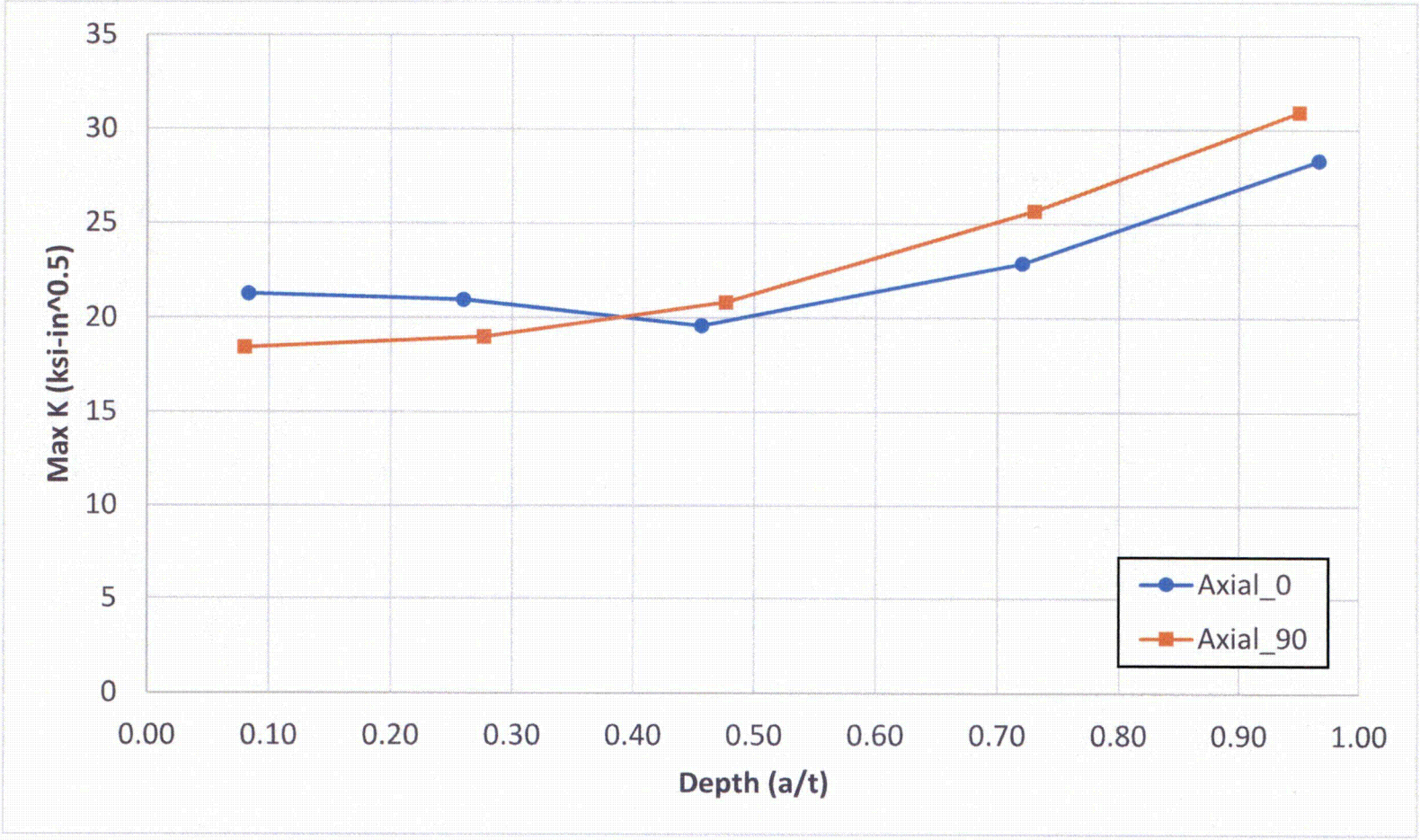

Figure 21. Stress Intensity Factors as a Function of Depth for the Bounding Cold Leg Nozzle Axial Flaws

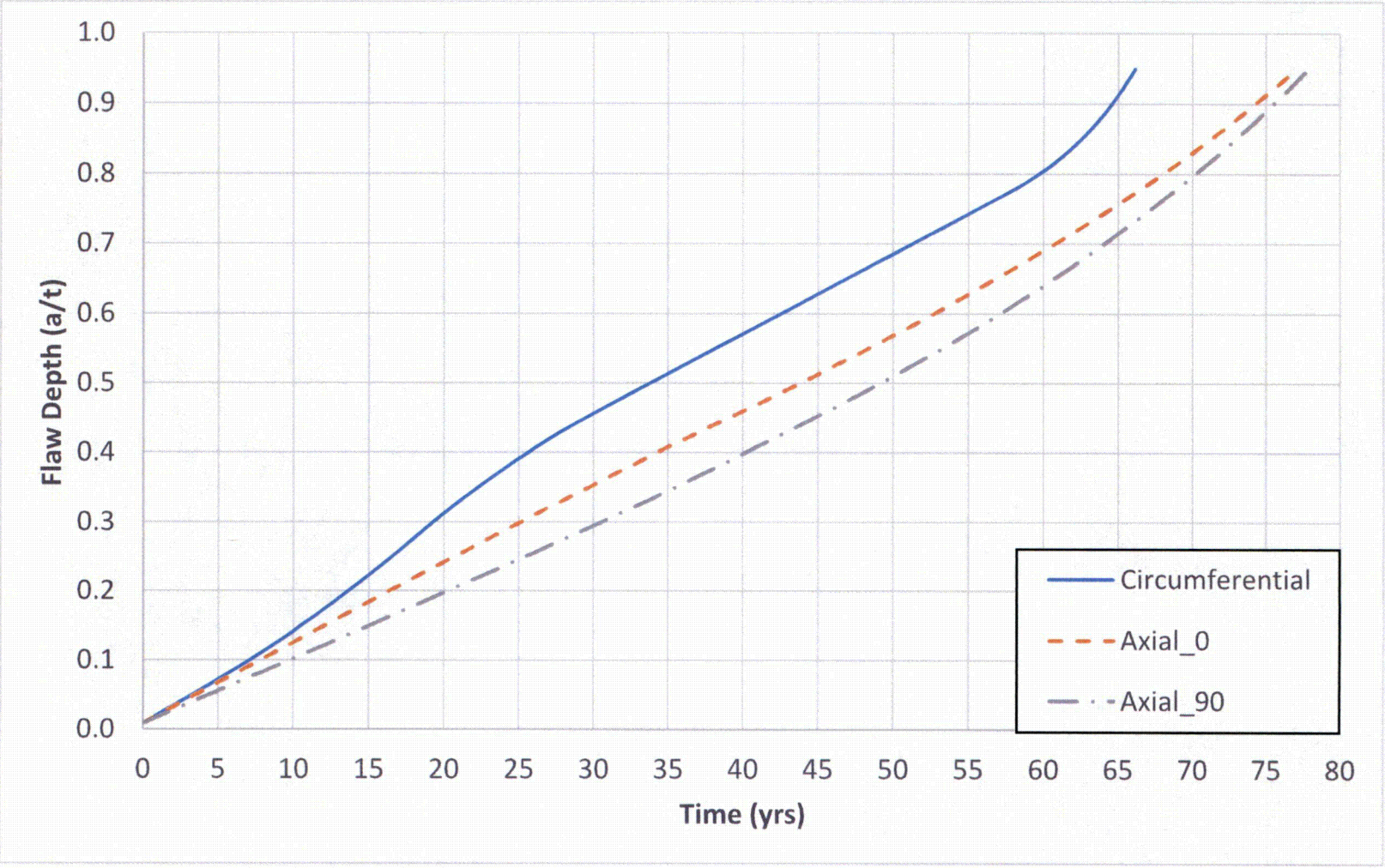

Figure 22. Crack Growth for All Flaw Types in the Bounding Cold Leg Nozzle (Initial Flaw of 0.025")

Attachment A
Crack Initiation Study

Introduction

The crack growth evaluations performed for relief request RR 4-18 did not include any calculation of initiation times for the hot leg drain nozzle. The evaluations only included a crack growth evaluation starting from day one of operation of the plant. This is conservative as some time is required for cracks to initiate prior to PWSCC growth occurring. This section calculates initiation time for the hot leg drain nozzle and the bounding cold leg nozzle using the module developed for the xLPR program. The xLPR program is a joint venture between the industry and the NRC to address the extreme low probability of rupture for Alloy 82/182 piping welds in PWR plants.

Initiation Model

xLPR reviewed a number of initiation models as part of the program. The xLPR Version 1.0 code used one model that was benchmarked for use on Alloy 82/182 weld material. The model used was named Direct Model 2 and was developed by EPRI in Report No. 1019032 [2]. It was benchmarked for use for Alloy 82/182 material and the inputs for use are in the xLPR Version 1.0 report by EPRI [1]. The model calculates the initiation time based on the material properties (yield and ultimate strength), temperature, and surface stress. The model also has two threshold stresses. The first is the stress initiation threshold (σ_{th}) where if the surface stress is less, no initiation will be predicted. The equations below calculate this initiation threshold. All equations presented in this section are rearranged from those provided in Reference 2 for ease of use and presentation.

$$\sigma_{th} = z\sigma_{ys}$$

$$z = z_1 + z_2 \ln(\xi)$$

$$\xi = \frac{\sigma_{ult}}{\sigma_{ys}}$$

where

σ_{ys} = local yield stress (input)

σ_{ult} = local ultimate stress (input)

z_1, z_2 = CW-SCC threshold parameters (input)

Additionally, there is a maximum stress (σ_{max}) where initiation would occur instantly. This value is calculated using the following equations.

$$\sigma_{\max} = D\sigma_{ys}$$

$$D = v \cdot e^{w \cdot \zeta}$$

$$\zeta = \frac{\sigma_{ult}}{\sigma_{ys}}$$

where

v, w = cold work microcracking resistance parameters (input)

For the evaluation documented herein, the stresses are between the minimum and maximum threshold values. Therefore, the time to initiation is calculated using the following equations.

$$t_{INI,nom} = BGe^{Q/RT} \ln\left[\frac{D-z}{\frac{\sigma}{\sigma_{ys}}-z}\right]$$

where

$$G = m^{-q}\frac{\ln(D)}{\ln\left(\frac{D-z}{1-z}\right)}$$

$$D = v \cdot e^{w \cdot \zeta}$$

$$z = z_1 + z_2 \ln(\zeta)$$

$$m = k\left(\frac{\sigma_{ys}}{E}\right)^a (\zeta - 1)^b (\zeta)^c$$

$$\zeta = \frac{\sigma_{ult}}{\sigma_{ys}}$$

and

$t_{INI,nom}$ = initiation time under fixed set of conditions (output)

T = temperature (input)

σ	=	surface stress (input)
E	=	local elastic modulus (input)
Q	=	activation energy for initiation (input)
R	=	universal gas constant (input)
B	=	proportionality constant (input)
q	=	environment-cold-work exponent (input)
a,b,c,k	=	general cold work parameters (input)

The inputs for the Palisades specific configurations are given below. Note that approximate values are taken for some of the physical properties of the material (E, yield strength, and ultimate strength). The actual values are close, and the differences here lead to insignificant changes in the results. The B value is a distribution in the Reference 1 report as xLPR is a probabilistic program. For this deterministic analysis, a conservative value was taken by using the 95% lower bound based on the inputs in Reference 1 (Appendix D).

The B value is a log normal distribution with values given below [1, Appendix D]:
Mean = 1.20e-9 hours → 1.37e-13 years (is equal to e^-29.62)
Standard deviation (heat to heat) = 1.607
Standard deviation (within heat) = 0.555
Overall standard deviation = $\sqrt{1.607^2 + 0.555^2} = 1.70$
The 95% percentile is 1.65 standard deviations away from the mean.
95^{th} = -29.62 – (1.65*1.70) = -32.425 → e^-32.425 = 8.3e-15 (in units of years)

T = 583°F (hot leg) (from body of report)
T = 537°F (cold leg) (from body of report)
Hot Leg Circumferential Surface Stress = ~41 ksi (see Figure 8 in the body of this report)
Cold Leg Circumferential Surface Stress = ~45 ksi (see Figure 12 in the body of this report)
E = 29e6 psi [3, at approximately 583°F (Hot Leg) and 537°F (Cold Leg)] the actual value at the operating temperatures are slightly below 29e6 psi. The difference will have an insignificant impact on the results.
Q/R = 22,000 K [1, Appendix D]
B = 8.3e-15 years (calculated above)
q = 0.375 [2, Table 5-4]
a = 0.25 [2, Table 5-4]
b = -0.75 [2, Table 5-4]
c = -0.25 [2, Table 5-4]
k = 10 [2, Table 5-4]
z_1 = 0.35 [2, Table 5-4]
z_2 = 0.333 [2, Table 5-4]
v = 0.66 [2, Table 5-4]
w = 0.5 [2, Table 5-4]
Yield Strength = 32,000 psi used (30,000 psi is the approximate value at 583°F (Hot Leg) [3] and 30,200 psi is the approximate value at 537°F (Cold Leg) [3]). Using 32,000 psi is conservative as it reduces the time to initiation.
Ultimate Strength = 80,000 psi [3, at approximately 583°F (Hot Leg) and 537°F (Cold Leg)]

Calculations

The model was used with Palisades' specific information to calculate the time to initiation. For the hot leg drain nozzle, the surface stress of 41 ksi (shown in Figure 8, page 15 of this report) and the hot leg temperature are used in the model to calculate the time to initiation. Figure A-1 shows the plot for this case. The plot shows the initiation time for a given surface stress. For the 41 ksi stress of the hot leg drain nozzle, the initiation time is roughly 130 years.

For the bounding cold leg nozzle, the surface stress of 45 ksi (shown in Figure 12, page 19 of this report) and the cold leg temperature are used in the model to calculate the time to initiation. Figure A-2 shows the plot for this case. The plot shows the initiation time for a given surface stress. For the 45 ksi stress of the bounding cold leg nozzle, the initiation time is roughly 600 years, 4.6 times longer than the hot leg drain nozzle despite the slightly higher surface stress.

For comparison, various different temperatures are considered to put the hot leg drain nozzle and bounding cold leg nozzle in perspective with other typical PWR plant components that have seen actual cracking in the industry.

The Palisades hot leg temperature is fairly low when compared to other PWR plants in the industry. Other PWR plants typically operate at a hot leg temperature above 600°F. For comparison, a hot leg temperature of 604°F is evaluated and compared to the hot leg drain nozzle at Palisades. The results of this comparison are presented in Figure A-3. Additionally, the hottest plant components are more susceptible to cracking. For PWR plants, susceptible locations exist in the pressurizer that operates at around 653°F. Figure A-4 shows the plot for initiation at the pressurizer temperature.

It should also be noted that most locations that have experienced cracking in the industry did not receive a PWHT. Therefore, the residual stresses for these other locations would have higher residual stresses, on the order of ~50 – 60 ksi. Looking at these higher stresses from the hot leg or pressurizer initiation plots shows that the time to initiation for these locations would be roughly 30 and 5 years for the hot leg and pressurizer, respectively (approximate values taken at 55 ksi surface stress).

Using the Palisades hot leg drain nozzle surface stress (41 ksi) for comparison, the higher hot leg temperature of 604°F would reduce the time to initiation by a factor of over 2 when compared to the Palisades temperature (~130 years vs. ~60 years). Comparing the Palisades hot leg drain nozzle results to a pressurizer temperature shows a factor of ~10 for time to initiation (~130 years vs. ~12 years). This shows the extreme temperature dependence related to initiation. For the Palisades hot leg drain nozzle, the lower temperature gives the location at least a factor of 2 over other hot leg locations in PWR plants.

References

1. *Materials Reliability Program: Models and Inputs Selected for Use in the xLPR Pilot Study (MRP-302),* EPRI, Palo Alto, CA: 2010, 1022528.
2. *Stress Corrosion Cracking Initiation Model for Stainless Steel and Nickel Alloys: Effects of Cold Work,* EPRI, Palo Alto, CA: 2009, 1019032.
3. ASME Boiler and Pressure Vessel Code, Section II, Part D, "Material Properties," 2004 Editions with no Addenda.

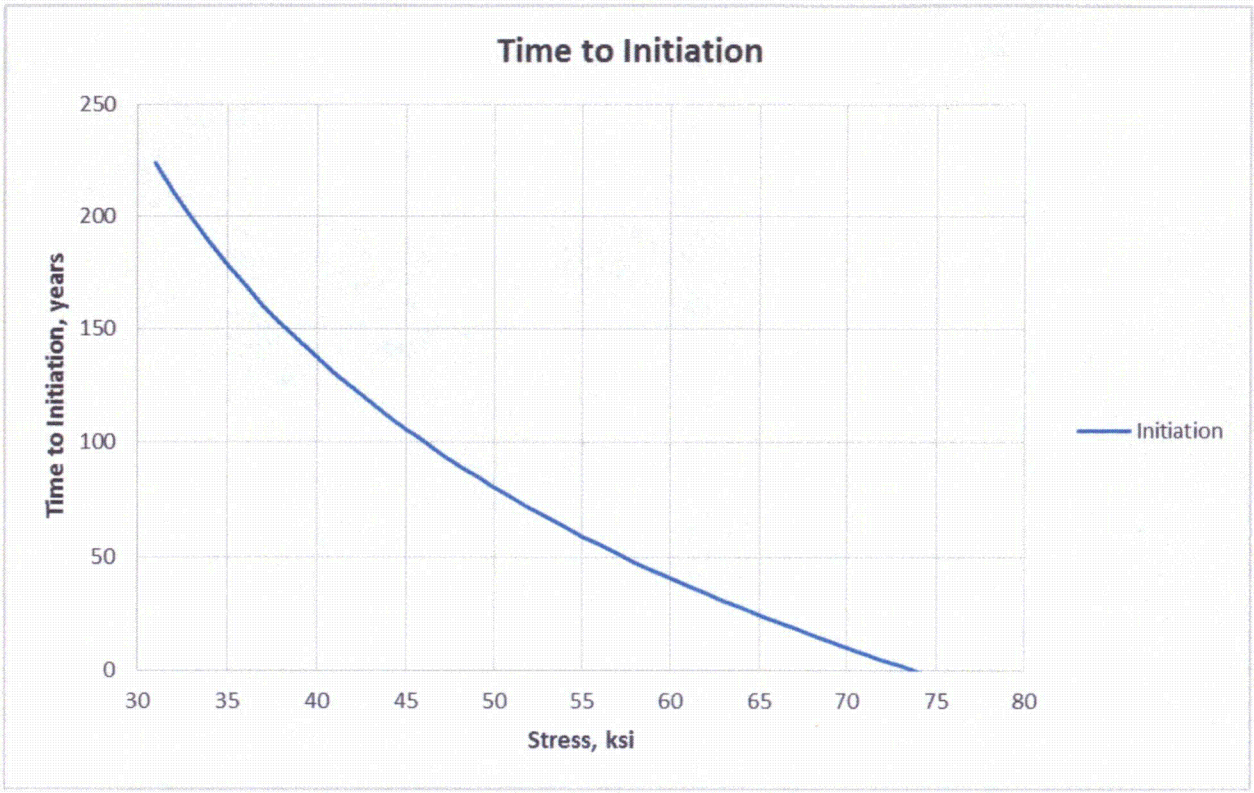

Figure A-1. Initiation Time for Palisades Hot Leg Drain Nozzle at the Hot Leg Temperature of 583°F

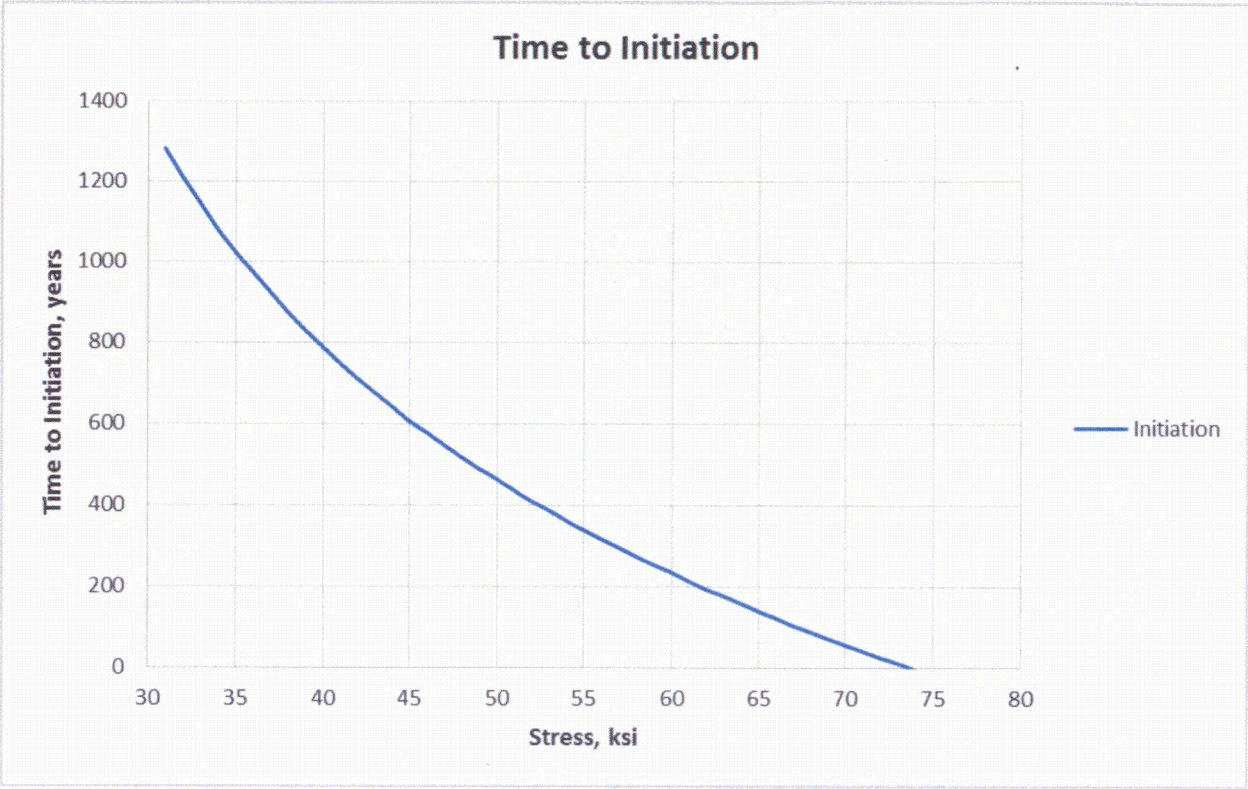

Figure A-2. Initiation Time for Palisades Bounding Cold Leg Nozzle at the Cold Leg Temperature of 537°F

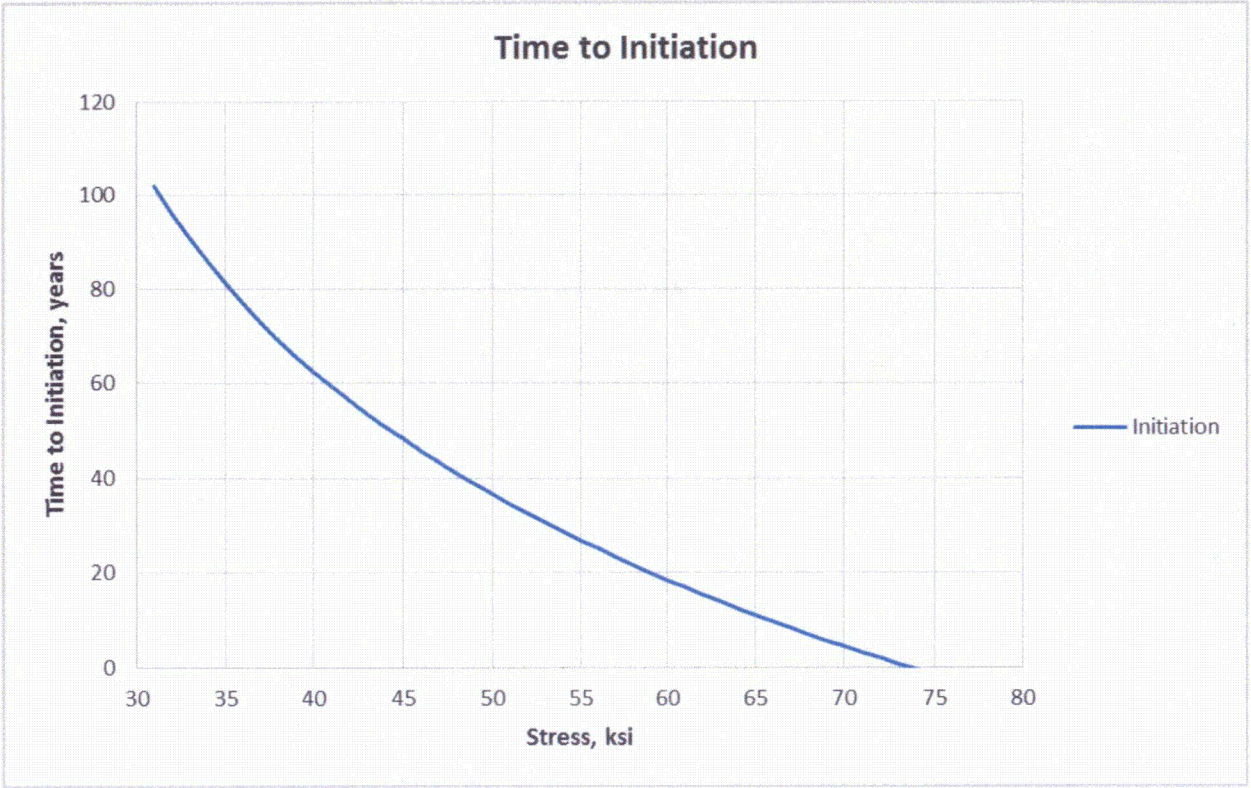

Figure A-3. Initiation Time for Typical Hot Leg Temperature of 604°F

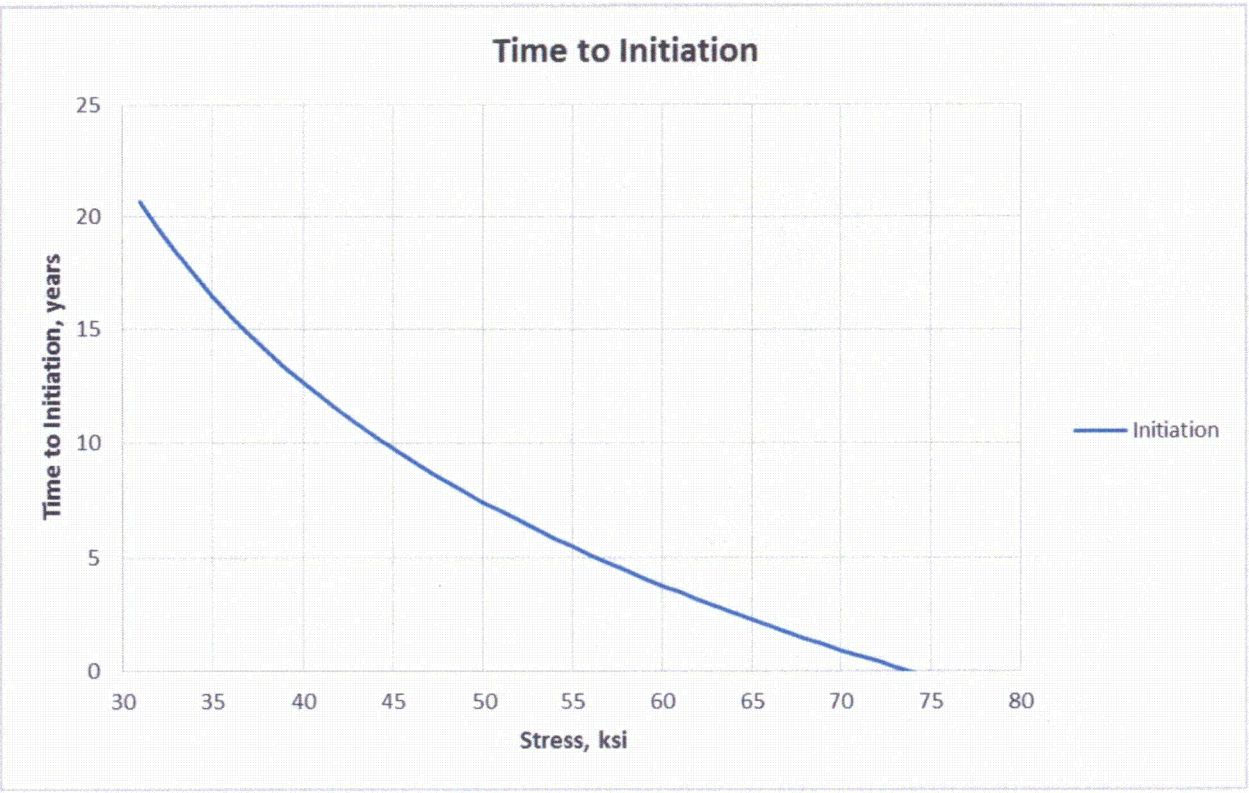

Figure A-4. Initiation Time for Typical Pressurizer Temperature of 653°F